LASER HARDENING OF EUTECTOID STEEL

by

SANJAY KUMAR DEO

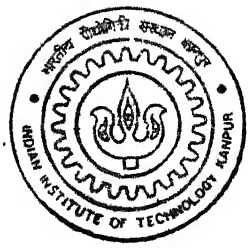

DEPARTMENT OF MATERIALS AND METALLURGICAL ENGINEERING
Indian Institute of Technology Kanpur

February, 2001

LASER HARDENING OF EUTECTOID STEEL

A Thesis Submitted
in Partial Fulfillment of the Requirements
for the Degree of

MASTER OF TECHNOLOGY

by

SANJAY KUMAR DEO

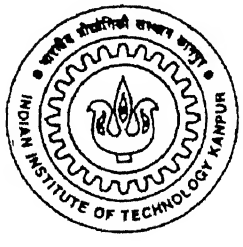

to the

DEPARTMENT OF MATERIALS AND METALLURGICAL ENGINEERING
INDIAN INSTITUTE OF TECHNOLOGY, KANPUR
February, 2001

CERTIFICATE

This is to certify that the work contained in the thesis entitled "Laser Hardening Of Eutectoid Steel", by Mr. Sanjay kumar deo has been carried out under my guidance and that this work has not been submitted elsewhere for a degree.

Dr.R.C.Sharma
Department of Materials and Metallurgical Engineering
Indian Institute of Technology,
Kanpur

Feb , 2001.

ACKNOWLEDGEMENT

With a profound sense of gratitude, I express my sincere thanks to my esteemed teacher and thesis supervisor Dr. R. C. Sharma for his invaluable guidance and encouragement throughout this work. I am indebted to him for providing me all the facilities and help in every possible way at IIT Kanpur.

I would also like to gratefully acknowledge Dr.Bansilal, Mr.M.Singh, Mr.Kuldip Singh and Mr.H.C.Shrivastava, who has helped me through out the experimental work, carried out in the laboratory. Thanks are due to all my friends who have made my stay at IIT Kanpur, a memorable and pleasant. Prominent amongst them is Amit, Santosh, Binod, Projit, Mantu,J k jain, and Pramod. Finally, I thank Mr. M.N.Mungole for his good company.

&

Last but not least, I would like to thank my parents and family members, who have been a constant source of moral encouragement and inspiration to me.

ABSTRACT

In the present work, surface hardening of eutectoid steel has been done by using a 150-Watt CO_2 laser. Variables like beam power density and scan speed has been used to optimize the hardening process. Experiments are done at fixed scanning speed but different beam density and vise-versa. Single hardened tracks are obtained by transferring the sample at fixed speed under the laser beam. Width and depth of the transformed (hardened) regions are measured by optical microscope. It is observed that at low scanning speed and focused beam condition, groove formation occurs near the surface. By defocusing the beam, the groove formation is removed. Hardness of the transformed region is ~ 950Hv, as compared to hardness of original matrix which is ~350Hv.

Hardened depth in the range of 50-810μ m could be obtained by using 150 Watt CO_2 laser. Hardened depth decreased, with increase in scan speed and beam defocusing. However there is an increase in width of the hardened region. No hardening occurs at scanning speeds higher than a certain value for given beam conditions. At higher defocusing of the beam, lower speed is required to obtain the same depth of hardening. No hardening is observed beyond certain defocusing at any speed.

To obtain continuous hard surface, overlapping of the single hardened track is done. Next to the overlapped regions, there is some decrease in hardness within the transformed regions. This variation is due to the tempering of martensite in heat-effected regions.

List of Figures:

LIST OF TABLES:

CONTENTS

CHAPTER 1

INTRODUCTION

Laser produces high intensity beam of light that is highly collimated with high wavelength purity. These properties enable the beam to focus to a size comparable to the wavelength of light, producing very high radiation density at focused spot. CO_2 laser is most commonly used laser in industrial applications. Its utility derives from the high power that can be generated at a wavelength of 10.6μm(i.e. infrared) suitable for processing a great variety of materials. Due to very high efficiency of CO_2 lasers, they are extensively used in all engineering applications and processing like, cutting, drilling, annealing, welding etc. and in areas like optical fiber drawing, laser isotope separation and laser induced fusion etc.

In the present work 150-Watt CO_2 laser has been used for surface hardening of Eutectoid steel. Hardening is a heat treatment process in which steel is heated to a temperature above the critical point, held at this temperature and then rapidly cooled. In this way the layer adjacent to surface can be transformed into austenite. High power laser has potential, as tools for the surface hardening of steels. By adjusting the varies parameters like power density, beam radius and scan speed one can obtain a desired depth of hardening regions. Self-quenching is due to conduction of cold metal beneath. Due to high cooling rate surface transforms from austenite to martensite.

Surface hardening is done to improve wear and abrasion resistance of parts designed to operate in friction. The hardening response of steel to laser treatment is primarily dependent upon the prior microstructure of the steel. Fine pearlite structures are preferable, because of small interaction time. Laser hardening is an alternative to flame and induction hardening. It has many advantages over other hardening methods, such as no external quenching is required and beam can easily reach the inaccessible areas of components. In most hardening processes the surface generated needs some

kind of post machining like grinding and honing, but laser hardening can be the final process as there is less heat input and hence less thermal distortion.

Eutectoid steel has been used as the material for surface hardening. Experiments have been done to know the effect of scan speeds and laser power density. Transform (harden) regions depth and width has measured by optical microscope. Microhardness test has done to measure hardness of the transformed region. The results show that the process is dependent on variables like power density, scanning velocity and beam radius. To obtain a continuous hard surface, overlapping of the single hardened track has done. Next to the overlapped regions, there is a variation of hardness value. This variation shows, hardness value decreases and again increases. Variation is due to the tempering of martensite in heat effected regions.

CHAPTER 2

LITERATURE REVIEW

2.1 Laser and its some unique properties: -

Since its development, the laser has been hailed for a variety of potential applications The theoretical concept of the laser was first put forward by Schawlow and Towns in 1958 and in 1960. Maiman developed the first working laser. A verity of laser system has been developing science, but the development of multikilowatt continuous CO_2 laser, around 1970. Has greatly increased the commercial feasibility of lasers in metallurgy and materials processing. The availability of high power density, $> 10^6$ watts/cm^2, is a primary factor in establishing the laser as a useful tool in metal and materials industries.

Laser is a Light Amplification by Stimulated Emission of Radiation. Laser light differs from ordinary light in that it consists of photons that are all at the same frequency and phase. Laser converts electric energy into a high energy density beam of light through stimulation and amplification. Stimulation occurs when electron in the lasing medium are excited by an external source such as an electrical arc resulting in the emission of photon. The energy required to raise the electron from one energy state to another is provided by an excitation process or pumping. This is achieved by the lasing medium's absorption of energy from mechanical, chemical or electrical sources. The lasing medium typically contains ions, atoms, or molecules whose electrons are conductive to change in energy level. According to quantum mechanics, atoms or molecules in the lasing medium have discrete electron energy levels. Laser light is created by the transition from a higher to a lower energy level, and the wavelength produced is a characteristic of the lasing medium. At the beginning of the lasing process, photon emissions are random in nature. As each photon stimulates other excited electrons to emit photons, however, the new photon will have similar wavelength, direction and phase characteristics as the initial photon. A stream of photons with identical wavelength, direction and phase will be produced. The most striping properties of laser lights are its high degree of: -

Directionality: - It is the phenomenon by which light bends around sharp-edged objects. When ordinary light is projected over a distance, a substantial amount of diffraction or scattering of light occurs, resulting in a loss of light intensity as the distance from the light source increases. This is the advantage of laser beam over ordinary light, is that lasers produce beams with very limited diffraction. Therefore, a laser beam can be projected over a distance with little divergence of the beam. This property of laser light produces a directional energy source, which can focus a large amount of luminous energy on a small area.

Monochromaticity: - It implies that the range of frequencies emitted by the light source is small. This is evaluated by measuring the line width. Laser light typically contains a single or a few spectral lines of very narrow widths. The frequency of the e.m waves is given by,

$$\nu = (E_2 - E_1)/h$$

where, h implies Planck's constant and E_1 & E_2 are the two different energy levels, Fig. 2.1 shows this effect more clearly.

Radiance: - The radiance of a light source is the amount of power per unit area emitted by the light for a given solid angle. In addition, the beams possess low divergence, which cause them to be transmitted over a small solid angle. Thus laser light sources posse's extremely high radiance (Fig. 2.3 shows).

Coherence: - It refers to the relationship between electronic and magnetic components of an electromagnetic wave. When these components are aligned, then beam is said to be coherent. There are two types of coherences: - Spatial and Temporal coherence. Spatial coherence refers to the correlation of phase at different points in space at a single moment in time and temporal coherence refers to the correlation of phases at a single point in space over a period of time (Fig. 2.2).

In order for most lasers to operate, these basic conditions must be satisfied: -

(a) An "active medium" that is collection of atoms, molecules or ions that emit radiation in the optical part of electromagnetic spectrum.

(b) Condition known as "population Inversion" created by an excitation process called "Pumping"

(c) For true laser oscillation to take place from frame of "Optical Feedback" must be present in the system.

A laser exploits three fundamental phenomenon's, which occurs when an e.m wave interacts with a material, the process of Spontaneous & Stimulated emission and the process of Absorption.

Spontaneous Emission: -

If energy level 1&2 and their corresponding energies denoted by E_1 & $E_2 (E_1 < E_2)$. The two levels could be any two out of large set of levels possessed by the materials. It is assume that an atom of the materials is initially in level 2. Since ($E_2 > E_1$) the atom will tend to reach to level 1. Thus the corresponding energy

difference $(E_2 - E_1)$ must released by atoms. If this energy is delivered in the form of an electromagnetic wave, the process will be called spontaneous emission. It is characterized by the emission of a photon of energy, $hv = E_2 - E_1$, v implies the frequencies of the radiated waves and h implies the Planck's constant.

So, $v = (E_2 - E_1)/h.$

Stimulated Emission: -

If the atoms is initially in level 2 and an electromagnetic wave of frequency "v" is incident on the materials. Then there is a probability that this wave will force the atom to undergoes to transition $2 \rightarrow 1$. In this case energy difference $(E_2 - E_1)$ is delivered in the form of an e.m waves, which adds to the incidents one. This phenomenon is called Stimulated emission, fig 2.4b shows it.

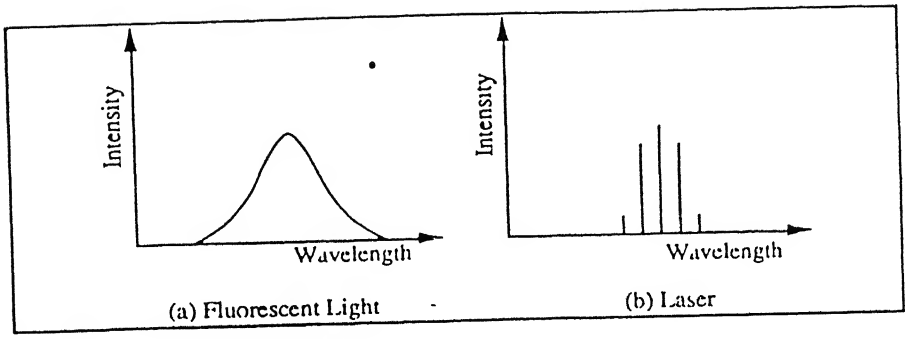

Fig. 2.1 Monochromaticity

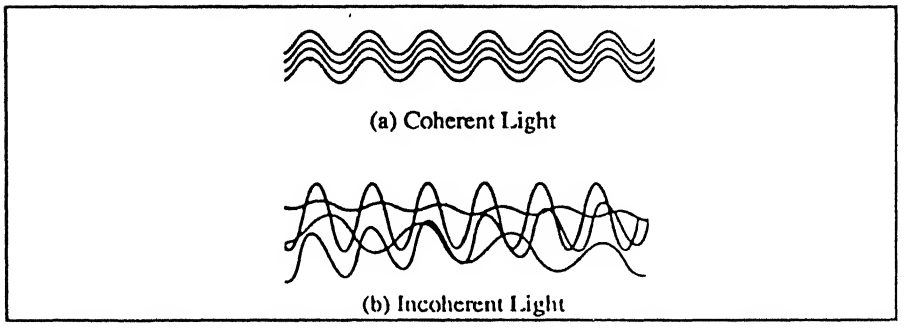

Fig. 2.2 Coherence

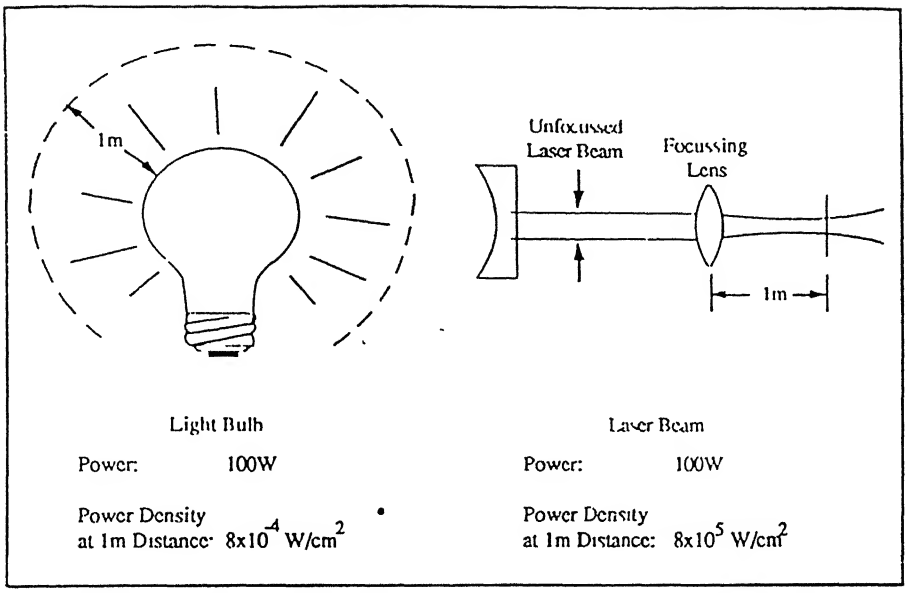

Fig. 2.3 Radiance

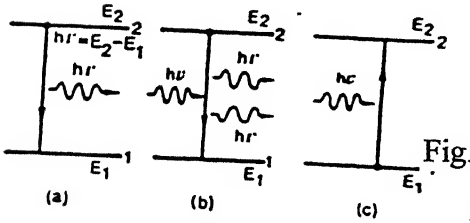

Fig. 2.4 Schematic illustration of the three processes: (a) spontaneous emission; (b) stimulated emission; (c) absorption.

Absorption: -

When atom is initially at ground level i.e. the level 1. Then the atom remains in this level unless some external stimulus is applied to it. If an e.m waves of frequency v is incident on the material, then the atom will be raised to level 2. The energy difference $(E_2 - E_1)$ required by the atom to undergo the transition to obtain from the energy of the incident e.m wave, fig.2.4c shows this thing. This process is called "Absorption".

The "Stimulation emission process" is an essential part of the operation of laser. When the laser is operating population inversion is automatically achieved. The "populations Inversion" regard for light amplification constituents an unequal distribution of atom among various energy levels. For example if we consider two energy level 1 & 2 of a given material and N_1 & N_2 are their respective population of atoms. The material behaves like an amplifier if $N_2 > N_1$, while it behave like an absorber if $N_2 < N_1$.

In the case of thermal equilibrium, the energy level populations are distributed Boltzmann statistics,

$$\frac{N_2^e}{N_1^e} = \exp\left[-\frac{(E_2 - E_1)}{kT}\right]$$

where, N_2^e & N_1^e are the number of electrons at energy states 1 and 2 respectively, E_1 and E_2 are the energy value for these states and T is absolute temperature.

2.2 CO_2-Laser: -

Laser equipment extensively employs CO_2 lasers in which the lower vibration levels of excited CO_2 molecules provide the mechanism for getting infrared radiation at a wavelength of 10.6μm. Most CO_2 lasers use a mixture of carbon dioxide, nitrogen and helium in different ratios to increase the power output. Adding nitrogen intensifies the lasing action. Helium features a high heat capacity and increased heat

conduction, so adding it speeds up heat removal, by they're reducing the mixture temperature [1]. The CO_2 laser can treated as a device transforms power one from to another with the efficiency n, which is given as the ratio of the output power to the input power,

$$\eta = (\text{Power output})/ (\text{Power Input}).$$

Operation of the CO_2 laser is based on the exchange of energy between the lowest-lying energy levels arising from rotation at and vibration at modes of the linear three-atom molecule. The upper limit on the efficiency of a CO_2 laser is 38%, which represents the quantum efficiency.

Generally, a CO_2 laser emission is limited to 20 % of the input energy, because of the sensitivity of the laser generating process to the temperature. The increase of temperature cause the increase in the number of hot CO_2 molecules, which cause the low energy levels to take place in the all heavy engineering applications and material processing like cutting, welding, drilling, annealing etc., and in areas like optical fiber drawing, laser isotope separation and laser induced fusion.

2.3 Laser In Metallurgy: -

During the past twenty years, both increasing demand for advanced materials and availability of these high power sources have stimulated considerable interest in research and development related to laser applications. The more obvious applications such as laser cutting, drilling, welding and heat treatment are already finding there way to industrial production lines. Laser offer an easily maneuvered. chemically heat source which can produce a narrow heat affected zone and low distortion. The use of laser for such applications as surface alloying, cladding, glazing and annealing of semiconductors offer the possibility of producing new materials with superior quality. Laser shock hardening is a process, which allows hardening of otherwise unhardenable materials. The inherent rapid rates of heating and cooling also open up the possibility for producing novel materials.

2.4 Laser Material Interaction: -

If a metal is irradiated with a short pulse of ultraviolet light, its interaction with the electromagnetic wave can be describe by the skin effect and the high-frequency conductivity. By means of Maxwell theory, it is possible to calculate a penetration depth of light wave as a function of the wavelength. The free movable charge carriers of the metals are shifted in the field of the electromagnetic wave. The generated electric current leads to heating according to the Joule effect. If the exposure time is long enough, this will cause heating, melting and evaporation. A further increase in the field strength causes field emission of electrons and finally result in plasma formation. What lies at the basis of any process of laser treatment is the ability of a laser beam to create a heat flux of high density in a small spot on the target surface.

The laser beam incident on the target is partially reflected from the target surface and partially absorbed in the surface layer 0.1 to 1μm thick by conduction electrons, which gain more energy and intensively collide with one another. At the initial time instant $t_1=10^{-11}$ s these electrons give small amount of absorbed energy to the crystal lattice of the metal, so the electron temperature T_0 of the metal considerably differs from the lattice temperature T_{inl}.

The energy transfer to the free electron crystal lattice grows in intensity with time. Starting at the relaxation time $t_{rel}=10^{-9}$ sec., the difference between temperature To and T_{inl}. Becomes metal can be acquired a common temperature T on the condition that the laser power density in the heat affected zone is not higher than 10^9 W/Cm^2.

The main share of laser induced heat propagates into the metal bulk by way of electron conduction [8], and so the laser induced thermal processes are similar in nature to conventional processes of metal heating. In most of cases the practical interest to absorbed radiation power density, varies in the bulk of a solid according to Bouguer's law

$$q_v(Z) = q_{vo}(1-R).\exp(-\alpha.Z)$$

where, $q_v(Z)$ and q_{vo} are the absorbed radiation powers per unit volume (in $Watt/Cm^3$)

the distance Z from the surface of the irradiated body and at its surface respectively, (1-R) and α are the light absorptivity and absorption coefficient in cm^{-1} respectively.

The optical properties of the metals can be described in the framework of the classical free electron model according to which the light flux minus the reflected parts is fully observed in interaction with the conduction electrons in the surface layer 10^{-4} to 10^{-5}cm thick.

Fig. 2.5 illustrates the laser energy distribution in the steady condition of melting. The energy balance equations below establish the relationship between the E_l coupled from the laser to the target and other kinds of energy predicted by the beam in the interaction zone.

$$E_l - (E_{plo} + E_r + E_d) = E_c \quad (1)$$

$$E_{plo} = E_{p11} + E_{p12} \quad (2)$$

$$E_c + E_{p12} = E_m + E_{hc} \quad (3)$$

where, E_l is the laser energy of the focused beam, E_{plo} is the energy of the plasma-vapor plume, E_{p11} is the radiant energy emitted from the plume into the environment, E_{p12} is the fraction of plume energy absorbed by cavity walls through convaction and radiant exchange, E_r is fraction of laser energy reflected from the base metal and cavity bottom, E_d is the energy of disintegration particles blown off by the vapor-gas jet, E_c is the fraction of laser energy absorbed by cavity walls in the the process of electron-photon collisions, E_m is the energy of heat of the molten metal pool and E_{hc} is the energy of heat delivered to the base metal and parent metal by way of heat conduction.

The efficiency of laser energy transfer to a target depends on the effective absorptivity A_{eff}, which actually determines the net laser-beam absorption

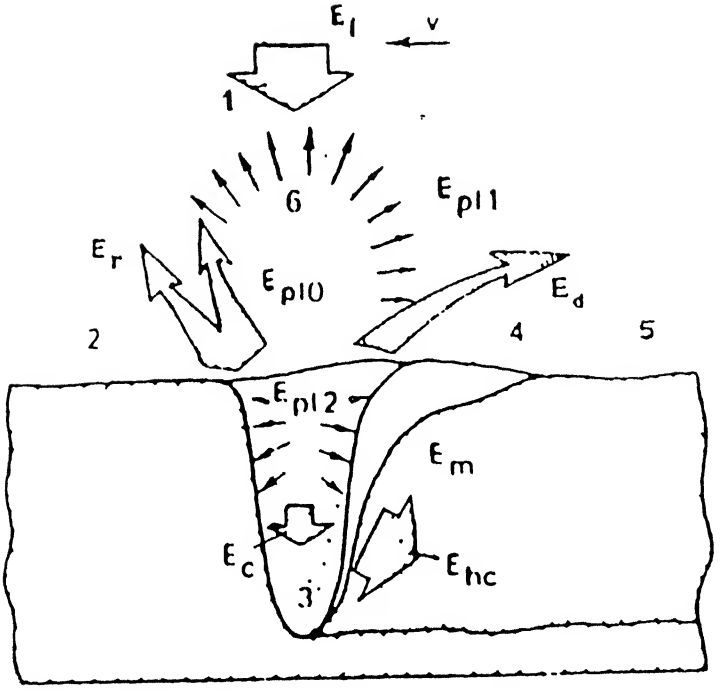

Fig. 2.5 Laser energy distribution in the study conditions of metal melting : (1) focused beam ; (2) base metal ; (3) cavity ; (4) liquid metal ; (5) weld metal ; (6) plasma plume.

efficiency η_η or coupling coefficient for laser radiation. An approximation for A_{eff} takes the from,

$$A_{eff} = \eta_\eta = (E_c + E_{p12})/E_1 \qquad (4)$$

Proceeding from theory of thermal processes in welding[8], we can express the laser beam absorption efficiency in terms of the net efficiency n_n given by equation(4). The effective heating power P_{eff} refers to the amount of heat that the beam of power P can deliver to a target in a unit time:

$$P_{eff} = n_n \times P$$

The net efficiency n_n defined earlier as the ratio of absorbed power to incident power characterizes the effectiveness of laser energy conversion and heat exchange. This coefficient has the same meaning as the absorptivity (A) in treatment without melting and as the absorptivity A_{eff} in heating with melting.

For the processes of laser heating with melting, the effective utilization of heat energy coupled to a metal target is defined by the thermal efficiency n_{th}, which is the ratio of the amount of heat required to melt a metal to the total amount of heat delivered to the metal target [9]:

$$n_{th} = (v.S_m.C_m)/P_{eff}$$

where, v is the speed of heat treatment, S_m is the cross-sectional area of a molten metal pool and C_m is the heat content per unit volume of a molten metal, including the latent heat of vaporization.

2.5 Conduction Of Heat In Metals :-

For understanding heat transfer by laser, we can examine the interactions between laser beam and material surface. First, the beam falls on the surface of material

and absorbs energy. This energy comes from the source like radiant energy. When the laser beam in impinges on the surface of the erosion front, portion of this energy may be reflected back to environment, transmitted into the workpiece interior or absorbed by the surface, this mode of heat transfer represent radiation heat transfer. Only fraction of total energy is absorbed by the surface rest energy is reflected to surrounding. The absorbed beam energy is transfer into thermal energy through lattice vibrations in the material An increase in the lattice vibration results in an increase in the temperature at the location. When the local temperature reaches the melting or vaporization temperature, phase changes will occurs. Some of the absorbed thermal energy may be transferred to atoms in the workpiece interior through lattice vibrations, this effect is called conduction heat transfer mode. Thermal energy may also be dissipated from the surface under the influence of fluid flow, this interaction's is called convection heat transfer mode.

Because the metal absorptivity and reflectivity is main criteria during heating. The heating rate of a metal sample is mainly determined the sample absorptivity of the metal itself and of the sample surface as well as the temperature range. The absorptivity (A) is the ratio of the intensity absorbed by the sample (Ia) to the incident intensity (I). At a certain moment in the process of laser heating, this is related to reflectivity (R) by, R= (1-A).

2.6 The laser heating source :-

Although the energy distribution in a cross- section of the laser beam may differ from case to case. But in general practice it is assumes that it follows Gauss distribution, in this case corresponding to monomode laser radiation are shown in the fig. 2.6. We write it

$$I(r) = I_0 \cdot \exp\left[\frac{r^2}{\left(R_s^e\right)^2}\right]$$

Where, I(r) & Io are the energy at difference distance, r is beam radius R_s^e is the radii within the irradiation spot at which the radiation intensity is e times lower then the maximum value.

The heat conduction equation :-

Let's us assume that the metallic sample is a homogeneous and isotropic medium. We shall consider the surface influence only through the changes in absorptivity. Then in case of semi-infinite simple,

Heat conduction equation,

$$-K\frac{\partial T}{\partial z} = AI_0 \qquad \text{(Heat flux at surface)} \qquad (6)$$

where, K = thermal conductivity

General conduction equation,

$$C(T)\cdot\rho\frac{\partial T}{\partial t} = \nabla[K(T)\nabla T] + G$$

where, C is the Specific heat/ volume, G is the internal heat generation source (Zero), ρ is the density of material.

So, $$C(T)\cdot\rho\frac{\partial T}{\partial t} = K(T)\nabla^2 T$$

$$\Rightarrow \quad \frac{\partial T}{\partial t} = \frac{K(T)}{C(T)\cdot\rho}\frac{\partial^2 T}{\partial z} = a\cdot\frac{\partial^2 T}{\partial z^2} \qquad (7)$$

where, "a" is the thermal diffusivity. Solution of the above equation (6) & (7),

$$T(z,t) = \left(\frac{2AI_0}{K}\right)\cdot\sqrt{at}\cdot ierf\left(z/2\sqrt{at}\right)$$

Here the coordinate z is directed into the sample, perpendicular to the sample surface, so that on the surface we have z=0. For z=0(surface temperature) the above equation is in

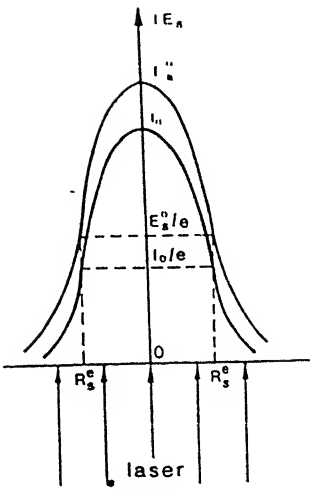

Fig. 2.6 Gaussian distributions of intensity, I, and of fluence, E_s, in a cross section of a laser beam.

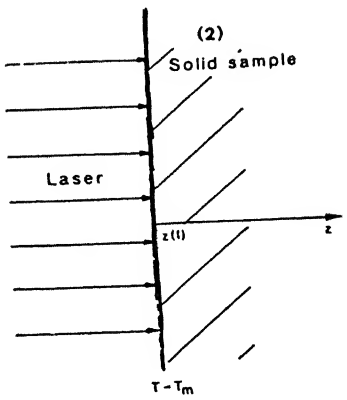

Fig. 2.7 Scheme for the laser heating of a solid (metal)

$$T(0,t)=\left(\frac{2AI_0}{K}\right)\cdot\left(\frac{at}{\pi}\right)^{\frac{1}{2}}$$

For very long heating duration $(t \to \infty)$, according to above equation the temperature increase to the surface $T \approx \sqrt{t}$.

2.7 Laser Surface Hardening Of Steel :-

Laser surface hardening (heat treatment) is the process of laser heating of a metal surface to a depth required for hardening and subsequent self-quenching of the surface layer at a high rate of cooling by heat conduction into the bulk metal. In distinction from the conventional processes of induction hardening, electric hardening or metal-bath hardening, laser hardening involves heating of the target surface to a shallow depth. The process of laser hardening entails specific structural transformations because of very high rates of heating and cooling.

Mechanism of Hardening in Iron-Carbon Alloys :-

The hardening of steels leads to the formation of an austenitic structure during heating and subsequent transformation of austenite into martensite at stage of cooling [13]. In surface hardening through solid phase transformations, the stage of heating determines the structural changes at the stage of quenching. On heating iron alloys to a critical point Ac_1, pearlite begins to convert to austenite at constant temperature if heating occurs at a slow rate.

Since the laser heats up the metal at a high rate, the pattern of austenite formation is different showing in Fig.2.8. The heat energy delivered to the metal exceeds the amount of energy required to rearrange the crystal lattice at a definite speed. For this reason, the transformation occurs in the temperature range between the starting point

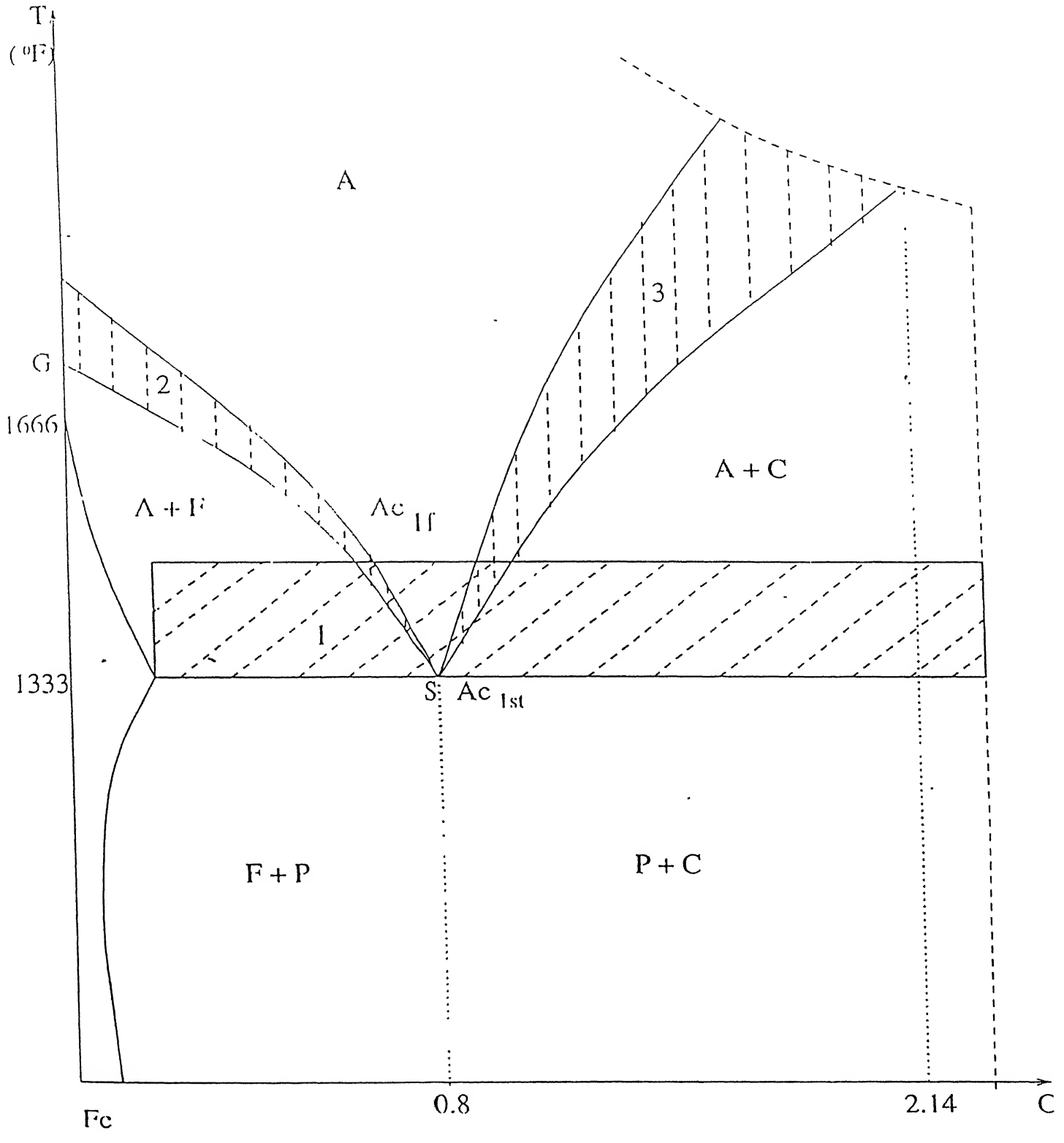

Fig. 2.8 Portion of the constitution diagram of Fe-Fe_3C for illustration of structura transformations on high-rate heating

Ac_{1st} and the finishing point Ac_{1f} rather than at constant temperature, i.e., in region 1 of high temperature [8].

Because of high heating rate, the diffusion process of conversion of excessive body-centered cubic ferrite (F) to face-centered austenite (A) may not terminate on line GS of the constitution diagram but shifts to region 2 of high temperatures. In a similar way, the fusion boundary between cementite (C) and austenite may shift within region 3. The process of diffusion redistribution of carbon in austenite, or diffusion annealing, shift to the region of still higher temperatures. The laser-hardened structure depends on the degree of completion of the austenization process that is governed by the heating rate, heating temperature, interaction time and the initial structure. At a high heating temperature and a sufficiently long interaction time slow substrate speed, the process may yield homogeneous austenite. A decrease in both the heating temperature and the interaction time slows down the homogenizing process and results in rather inhomogenity of the initial structure.

An increase in the heating rate in grain refinement, but the process of austenite formation is complicated by the effects of restoration of the grain shape and size. In the process of heating and even during cooling, austenite grain grows, although the carbide particles that withstand high temperature inhibit the grain growth. Under these conditions the size of the austenite grain depends on the relationship between the heating temperature and the interaction time. Since the interaction time of the beam is short, the grain has no time to grow large. However, it is desirable to heat the metal up to its melting point in order to increase the depth of hardening. But in this case, the austenite grains cannot be too fine. Fine grains only form at the boundary of the laser-heating zone where the temperature is not high.

As noted above, a high cooling rate ensure self-quenching and hardening of the surface layer. To obtain martensite in iron-carbon alloys within the temperature range of from 673 to 873 K. Where austenite is least stable and the cooling rate should be exceed the critical values i.e, more than 150 K/sec. for most iron alloys. The cooling rate in transformation hardening is very high. An increase in the cooling rate does not

change the composition of phases and structures such as martensite, cementite (carbides), and retained austenite. But high cooling rates can be responsible for highly nonuniform structure due to inhomogeneous austenite and can lead to structural defects because of the enhanced precipitation hardening and retarded processes of recovery and recrystallization.

In the case of cooling, the portions get finer and the density of dislocations and the stresses of the metal grow. Laser hardening yields a finer martensite than that formed by conventional techniques. The microhardness of the laser- treated steels can be by 2000 Mpa higher than that of steels hardened by the conventional methods.

As mentioned above, surface hardening with melting (liquid phase quenching) affords heat treatment to a larger depth. The grain size decreases at a high cooling rate, but not in a unique fashion because the crystal growth rate and the nucleation rate very in a complex manner with overcooling, i.e, the difference in liquids and actual crystallization temperatures.

The cooling rates of 10^3 to 10^6 K/sec., dendritic segregation takes place. This process enriches the grain region solidification at the stare and the end of crystallization in high-melting and low-melting element, respectively. The cooling rates above 10^6 K/sec. Cause the formation of a flat crystallization layer, which retards the distribution of elements in the liquid phase, so that the dendritic segregation slows down sharply.

With an increase in the cooling rate, the concentration of a dissolved element in the solid solution grows in comparison with the equilibrium concentration and leads to the formation of a metastable (supersaturated) solution. At super high cooling rates, the crystallization centers have time to grow and the metal solidifies into a glassy mass with an amorphous structure that display a certain short-range order in the arrangement of atoms.

2.8 Structural Changes in Laser-Hardened Iron-Carbon Alloys: -

The laser beam heats up the metal target in depth to different temperatures, so that the laser-treated zone has a layer structure and consists mainly of three layers. The first layer is the hardened region formed by the melt, which, generally, has a columnar structure with crystals stretched in the direction of the heat removal. The structure mainly consists of martensite, carbide being commonly dissolved. In optional condition of hardening, decarburization does not occur and the layer is free of craters and slag inclusions. In solid phase transformation hardening, the structure does not contain the first layer.

The second layer is the hardening region formed from the solid phase, with its lower boundary determined by temperature of heating upto the critical point Ac_1.The layer is the region of both full and incomplete hardening. The structure is inhomogeneous in depth. The upper portion consists of martensite and retained austenite formed from homogeneous austenite at the stage of cooling. The lower portion contains, along with martensite, the elements of the initial structure, namely, ferrite in hypoeutectiod steel and cementite in hypereutectiod steel.

The third layer is the transition structure region formed in the metal after its heating to a temperature below the critical point Ac_1. In the steel initially hardened or tempered, layer of toorsite or sorbite is formed in the process of laser treatment, which has a reduced microhardness. This laminated structure is typical of steels heat-treated with CW pulsed lasers. Follows briefly the structure of some laser-hardened steel.

Hypoeutectiod Carbon Steels:

In low-carbon steels contain less than 0.3 percent carbon, the first liquid phase hardened layer consists of fine-needled martensite [4], the microhardness of which is comparatively lower.

The solid-phase transformation region exhibits a more inhomogeneous structure. The upper portion of the region treated with a pulsed laser or a CW laser at

high speeds may consist of martensite, which is formed in small areas of the formed pearlite. At a lower speed of CW laser treatment, the layer displays homogeneous plate-like martensite The lower portion of the layer includes coarse grains to ferrite, in general; laser hardening of low-carbon steels offers little promise for industrial applications.

In laser-treated medium-carbon steels containing up to 0.6 % carbon, the martensite hardness increases appreciably. In normalized steel treated with a CO_2 laser, the first liquid-phase hardened layer exhibits fine-grain plate-like martensite. The second solid-phase hardness is equal to that of the first layer and the lower portion of an inhomogeneous structure. The inhomogenity of the components in the lower portion changes in depth in the following sequence, martensite-toorsite, martensite and toorsite, toorsite-ferrite and ferrite at the boundary with the original structure.

In normalized or annealed steels laser-hardened at a high rate, the region of homogeneous martensite is absent and the toorsite-ferrite network around martensite may extend up to the surface, thus reducing the hardness [8]. For this reason, heat treatment must be carried at low rates, less than 10 mm/sec., with the beam dithered, where possible, to increase the region of homogeneous martensite. Laser hardening of steels preliminarily subjected to high-temperature produces the same feect.

Eutectoid and hypereudectoid carbon steel: -

In these steels laser-hardened with melting, the first layer consists of fine-grain martensite and retained austenite whose content can be as high as 45 %. Science undissolve cementite is absent, both martensite and austenite are quite rich in carbon. As a result, in steels containing 1.0 to 1.2 % C hardness of martensite increases.

In the second layer, the upper portion contains dissolved carbides and has the solid solution saturated with carbon, which leads to an increased content of retained austenite. The lower portion contains undissolved carbides and has a much lower content of austenite, which results in a maximum hardness of the structure. This necessitates

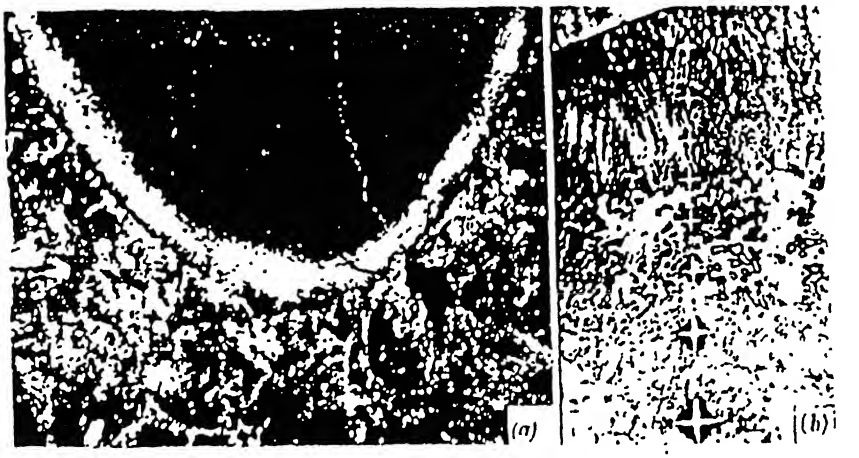

Fig. 2.9 Micrographs of laser irradiated zone in eutectoid steel
(a) X 200(initial structure of lamellar pearlite) ;
(b) X 600 (granular pearlite).

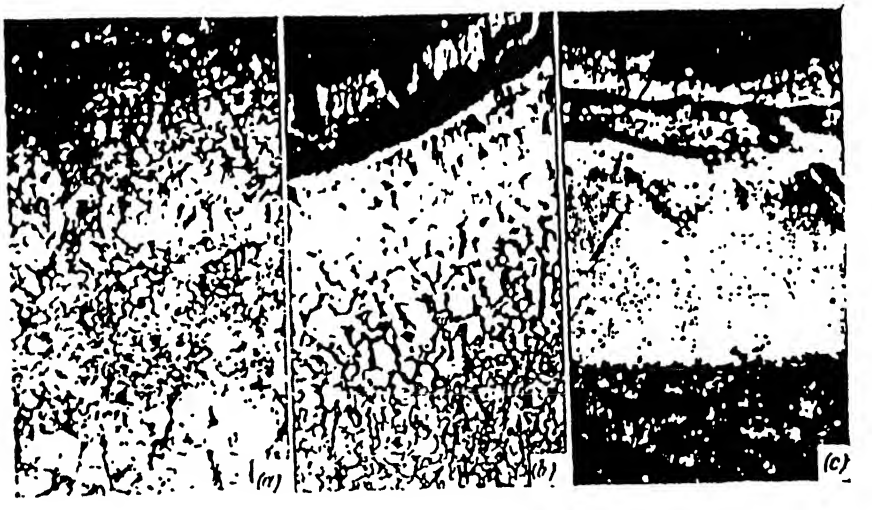

Fig. 2.10 Microstructures of zones irradiated with continuous-wave laser radiation
(a) X 150 (armco-iron) (b) X 150 (steel 45)
(c) X 150 (eutectoid steel).

hardening of hypereutectoid steels at highest speeds to import the hardened layer structure with undissolved carbides.

The first layer of the affected zone in eutectiod steel (Fig. 2.9) consists of acicular martensite and considerable amount of residual austenite. In the hardened layer adjacent to the molten layer the significant etching of grain borders is seen owing to segregation of impurities (Fig. 2.10).

Alloyed Steels:

The alloying elements of these steels exert diverse effects on the structure of the laser-treated zone. The microhardness of a low-carbon alloy steel after laser hardening is greater than that of laser-hardened unalloyed steel with the same carbon content. The hardness of laser-treated medium-carbon steels, containing even a small amount of alloying element increases appreciable. For example, the microhardness of chromium steel after CW laser hardening, which is much higher than that of laser-hardened carbon structural steel.

In high-carbon steels, small addition of alloying elements render the laser-hardened zone more inhomogeneous because of a decreased diffusivity of carbon and increased stability of carbides. In laser hardening of chromium steels, the liquid-phase hardened layer displays a fine-grain structure of high-carbon martensite and retained austenite. A high rate of laser hardening preserved carbides in the surface layer. The alloying elements add to the hardness of martensite in the layer formed from the melt. However, this layer generally exhibits microcracks, and therefore it is inadvisable to use laser hardening with melting for these steels.

The solid-phase hardened layer in laser-hardened chromium steels is inhomogeneous. Because of the incomplete process of austenizqtion at the heating stage, the portion of the layer contains martensite, undissolved cementite and retained austenite. In annealing steels, this portion has a low hardness. The middle portion heat-treated to higher temperatures exhibits high-alloy martensite and undissolved carbides,

which impart high hardness in the structure. The upper portion of the layer contains dissolved carbides this portion heats up to a high temperature, austenite homogenizes completely. After it's cooling, the metal of this portion transforms into fine-needled martensite and contains an increased amount of retained austenite of a relatively low microhardness.

Varying the parameters of heat treatment offers a means for control of individual regions of the laser-treated zone. A small interaction time ensures a partial dissolution of carbides that is sufficient to saturate martensite and simultaneously preclude an increase in the amount of retained austenite. Transformation hardening with a pulsed laser or a CW laser at a high rate can provide such a structure.

Varying the parameters of heat treatment offers a means for control of the individual regions of the laser-treated zone. A small interaction time ensures a partial dissolution of carbides that is sufficient to saturate martensite and simultaneously preclude an increase in the amount of retained austenite. Transformation hardening with a pulsed laser or a CW laser at a high rate can provide such structure.

High-alloy tool Steels: -

Since these steels display a low mobility of carbon, it is difficult to carry out laser hardening at an optimal degree of austenization, i.e., with minimum dissolution of the carbide phase and sufficient saturation of a solid solution. At a low laser power, austenite becomes saturated at the heating stage and so low-carbon martensite and retained austenite appears at the stage of quenching. In the process of surface hardening at a high laser power, the dissolution of carbide results in supersaturated austenite, which is responsible for a large amount of austenite in the hardened layer.

So, for each grade of high-alloy steels, it is necessary to a narrow range of heat treatment conditions so as to ensure the formation of martensite with a sufficient amount of carbon and preclude the dissolution of carbides to a certain extent at the heating stage. Both transformation hardening and surface hardening with minimum melting can provide this type of structure.

In laser hardening of die and high-speed steels, the hardened layer can acquire a high hardness. This layer hardened with a pulsed laser or a CW laser consists of martensite, carbides and a small amount of retained austenite. An optimal process of hardening with melting can be set up by properly selecting the pluse length or using the energy of a pulse that is 2 and 3 joules lower than the critical value. A CW laser can ensure a high hardness in the process of heat treatment with minimum melting.

2.9 Laser hardening variables: -

Metallurgical variable:

Laser surface hardening is similar to any other surface hardening method such as induction or flame hardening except that the laser beam is used to generate heat. The heating up to austenising temperature, particularly in laser heating, is very short-fraction of seconds. The dwell time cannot be made large as surface melting may occur which is undesirable. As the heating rate is very high, higher temperature is attained soon. The rate of austenisation is very fast, but the time of austenisation is too short. Thus the original microstructure of ferrous material should be very fine most preferably the hardened and tempered state. High peak temperature obtained by high-density laser beams result in more retained austenite in steels. The presence of large amount of retained austenite is not desirable.

Process Variable:

Some of the major process variables connected with laser heat treatment are incident laser beam power, diameter of incident laser beam, and absorptivity of laser beam by the substrate and transverse speed across the substrate surface. Another important factor in this context is thermo-physical properties of the substrate. The depth of hardness, geometry of the heat affected zone and the microstructure and metallurgical properties of the laser heat treated material are dependent variables.

For efficient laser heat treatment, it is necessary that proper absorption of light energy by the work-piece take place. All heat transfer calculations for processing

are based on this absorbed energy. With a given beam diameter and traverse speed, the depth of hardening by laser heat treatment is proportional to the laser power. The power density as also the coverage rate depends on the diameter of the laser beam. For laser heat treatment, a wide beam with uniform intensity distribution is preferable. This is ensuring uniform case depth.

The interaction time depends on traverse speed. The depth of hardening is inversely proportional to traverse speed. With the use of laser of high power density, the temperature gradient at the surface of component becomes steep. As melting of the surface is to be avoided or rather the peak temperature should be much less than this, the speed of laser spot has to be high. This limits the case depth obtainable. Fig. 2.11 shows the maximum temperature profile for high power, high speed and for low power, low speed lasers. Depths attaining temperature higher than A_3 is the case depth. Case depth is higher for low density, low speed laser [3]. A ferrous material having poor hardenability such as plain carbon steels are laser surface hardened by high power density and high travel speed. Lasers of lower power density have lesser temperature gradient at the surface and the temperature attained at the surface of component is less (than high power density) the dwell time of laser can be increased by decreasing the speed of the travel of laser spot. The relationship between depth of hardening and power is given by,

$$Y = -0.11 + \frac{3.02p}{\sqrt{D_n V}}$$

where,

Y = case depth (mm)

P = laser power (KW)

D_b = incident beam diameter (mm)

V = traverse speed (mm/s)

Laser heat treatment is best suited for steel and cast irons. During laser heating, heat transfer takes place by interaction of laser beam with the free electrons of

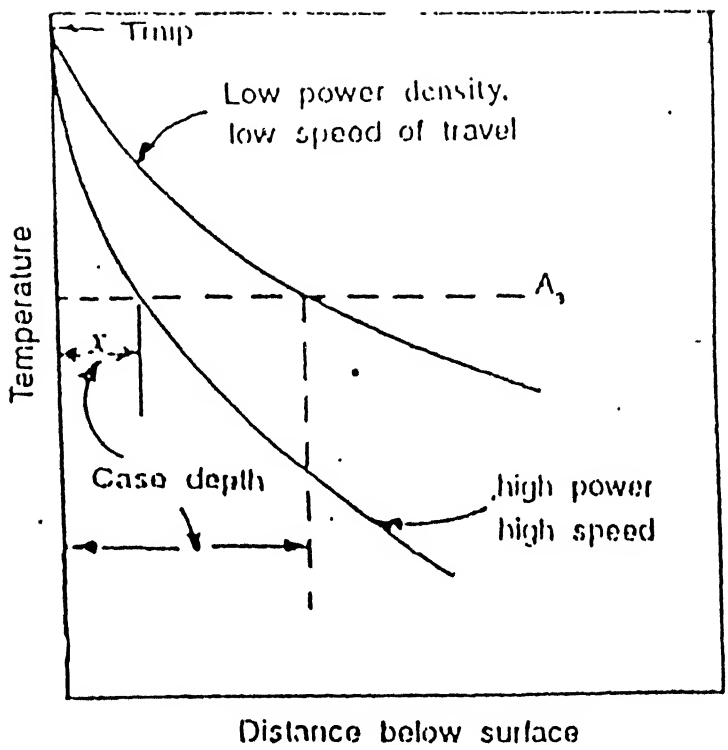

Fig. 2.11 **Maximum temperature profile for high power,high speed and for low power,low speed lasers.** [3]

the substrate. As a result, the energy state of the electrons of the conduction band is raised.

2.10 Advantages And Limitations Of Laser Hardening: -

Advantages: -

While considering laser heat treatment, it is necessary to apply the same metallurgical concepts as in the case of other conventional heat treating process. However, there are some basic differences between the laser heat treatment processes. The main advantages of laser heat treatment are as follows:

1 It is possible to harden low carbon steel (non-harden able steels like mild steels) with relative ease due to extremely rapid heating and cooling rates associated with laser heating. There is hardly any effect due to differences in hardenability between plain carbon steels and alloy steels since the cooling rates normally achieved during laser heat treatment are much higher than the critical cooling rate required for martensitic transformation.

2 Hardness obtained is slightly higher than conventional hardening.

3 It is possible to achieve high production rates since light has no inertia and consequently, it is possible to obtain high processing speeds with rapid stopping and starting.

4 No external quenching is needed. At times external quenching may be adopted for such small parts which have insufficient mass for self-quenching.

5 Close control over power input helps in eliminating dimensional distortion.

6 Beam (with the help of optical parts) can be easily reach the inaccessible areas of components, and re-entrant surfaces.

7 The last optical element of the laser and the component to be surface hardened may be far placed.

8 Very long and irregular-shaped components can be hardened easily.

9 Laser delivery systems are quite flexible.

10 No vacuum or protective atmosphere is required.

11 Entire process can be controlled by microprocessors.

12 Distortion is minimal.

13 Several jobs can be performed simultaneously with one laser using several working places each with its own optical system.

14 High productivity is obtained, as time is too small.

15 Normally no external quenching is needed, thus saves the problems related to coolants, storage, spilling and cost.

16 No final machining is required after hardening.

17 It is possible to give localized treatment by this method.

18 There are no flames, no contamination etc. in this process.

19 There could be precise control over the areas to be hardened.

Limitations: -

1 High installation cost for large laser.

2 Working cost is very high.

3 Lasers use maximum 30% of the input energy, which is inefficient.

4 Difficulties come in the case high alloy steels.

5 Extra care is needed to avoid fusion.

CHAPTER 3

EXPERIMENTAL PROCEDURES

3.1 SPESIMENS PREPARATION:

Starting material used in the present work was in form of Rail steel block. The normal composition of the steel corresponds to the eutectoid composition. In the first step, proper size samples were cut by abrasive cutter. The average size of the samples were (2cm× 1cm ×1cm). After that samples surface were made clean by emery paper.

3.2 LASER SETUP:

Experiment was done at a power of 150-Watt CO_2 laser, by using a high power 1.5 KW commercial lasers. Original capacity could not obtained due to some difficulties. Only 150-Watt, fix output was obtained by the system. So in present work, all experiment was done at that power. Laser is designed like V shape and total reflecting mirrors are connected at each end. So that the final output obtained at one end i.e. output end. System is fully automatic, fig. 3.1 shows one view of the system.

The traversing platform consists addition parts other then platform, a motor and a voltage controller. The voltage controller control the rpm of the motor and hence the traversing speed of the platform. Fig. 3.2 shows the schematic diagram of platform. There was a lower limit of voltage, below which no motion obtains. This was critical voltage of the motor. The lower value of platform speed, obtain was 2 mm/sec. The variation of the platform speed with the voltage is shown in fig. 3.3. This plot was used to read voltage required for any particular speed. There were two screw-gauges at top of the platform, which was perpendicular to each other. By the use of this screw-gauge, platform moved in either direction easily. They were used for moving the sample by small distance, in the case of overlapping.

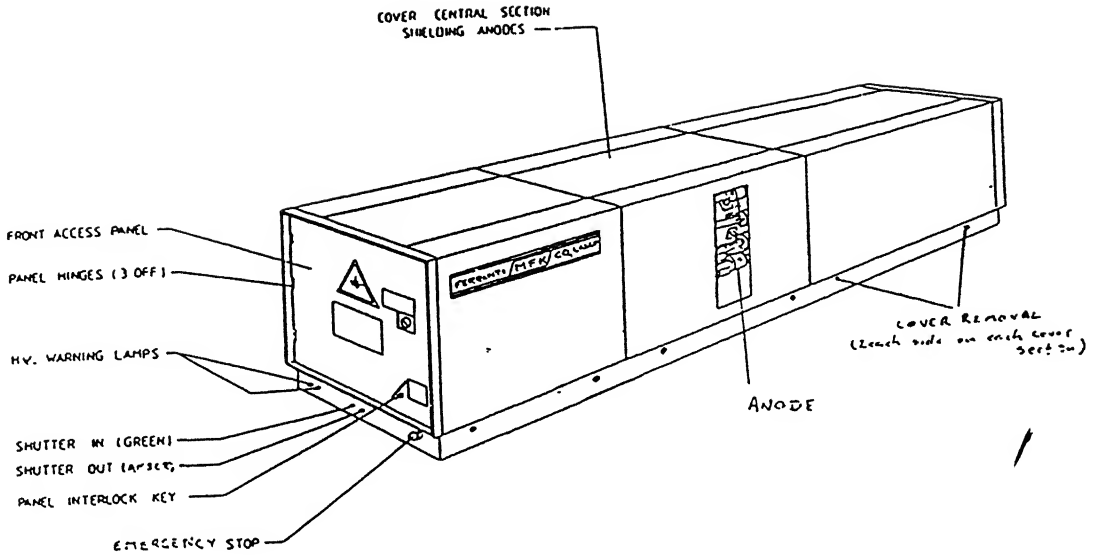

Fig. 3.1 LASER HEAD

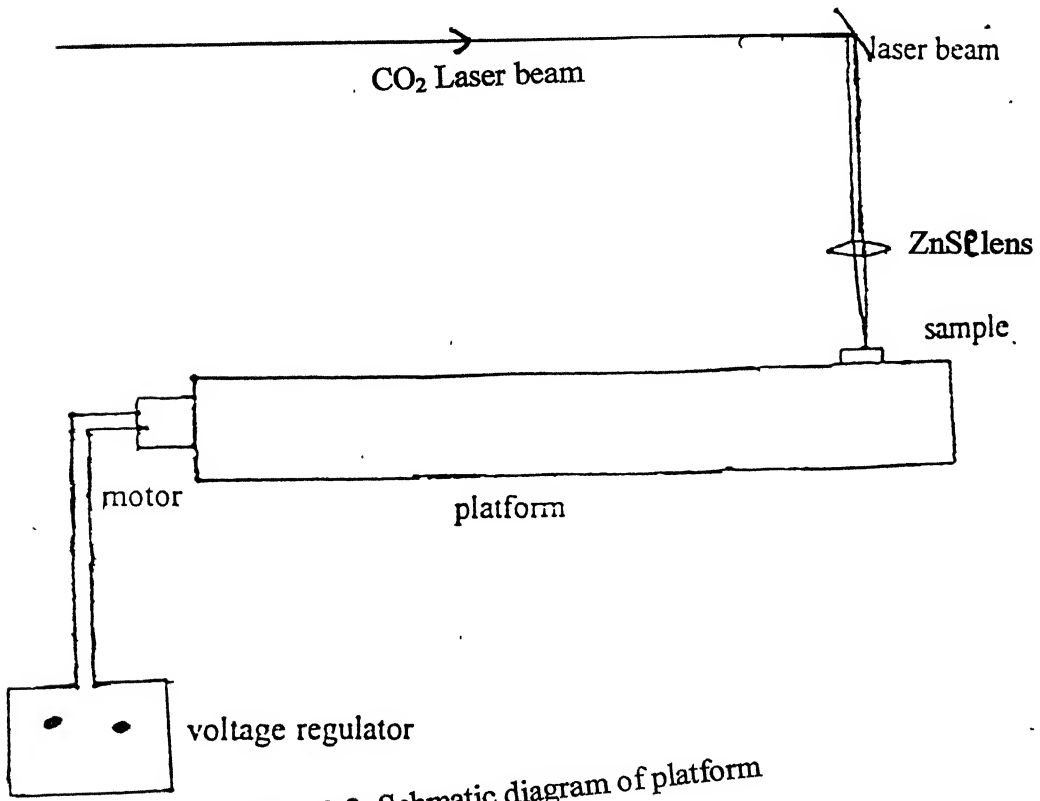

Fig. 3.2 Schmatic diagram of platform

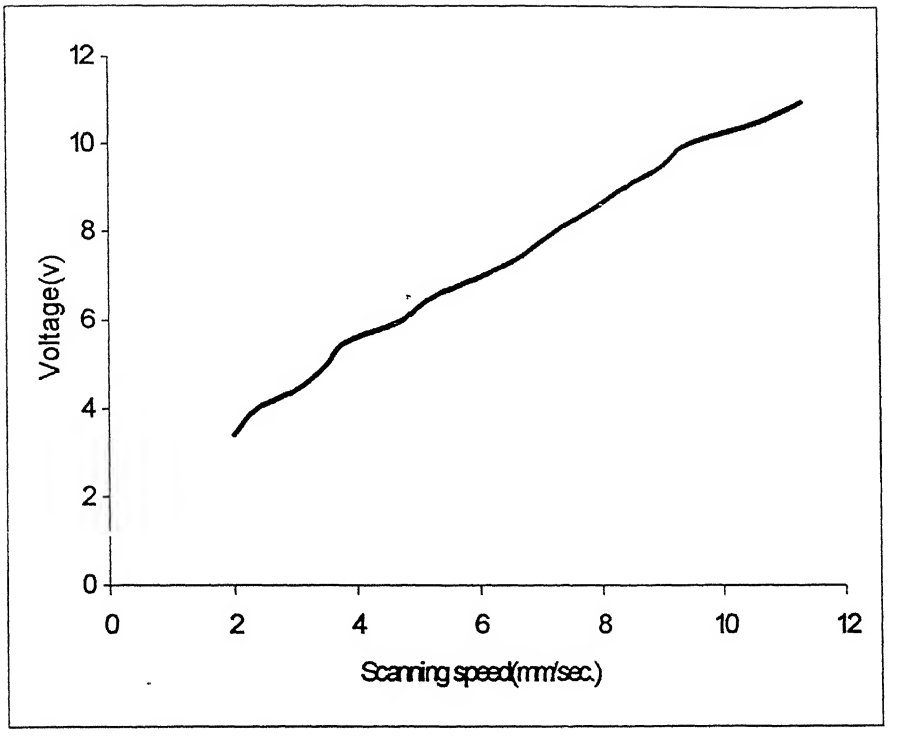

Fig. 3.3 Scan speed vs Voltage required for platform

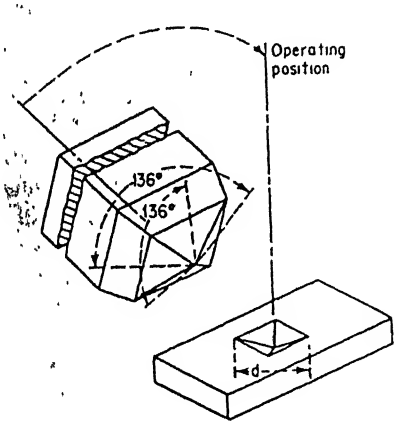

Fig. 3.4 Vicker's diamond-pyramid indenter

3.3 LASER HARDENING EXPERIMENTS:

During experiment platform was transvering at fix speed under the static laser beam. Speed of the platform was control by voltage controller. First sample was put on the top of the platform In between sample and laser output hole, there was a ZnSe lens. This lens was connected with screw-gauge so that it was easily moved up and down for focusing and defocusing purpose. It was very difficult to predict the exact focused position, therefore some experiments were done to decide the focused position, before the final experiment. Dimension analysis was done to decide the focused and defocused position. Accurate beam diameter measurement was not possible but relative focusing or defocusing diameter was easily obtained. First visually focusing the beam on the working sample surface and then defocused it by using screw gauge. As a process variable, different scan speeds were used. Table 3.1 shows the different variable used during the experiments.

To obtain continuous hard surface, overlapping of single-track transform regions was done. For this, fixed the other parameter and move the sample perpendicular to scan direction nearly 0.5 mm with the help of screw-gauge. Because in the previous experiment (single stack) it was found that, maximum width of the transforms region 1mm obtained by defocusing the laser beams. Hence to obtain a continuous hard surface just move the sample half the width of transformed region. Same processes were repeated 5-6 passes, and continuous hard surface was obtained.

Table 3.1: Process variable used during experiments.

BEAM CONDITION	PASSES	SCAN SPEED (mm/sec.)
Focused	Single	2, 4 and 6
0.3 mm Defocused	Single	2, 4 and 6

0.7 mm Defocused	Single	2, 4 and 6
1.0 mm Defocused	Single	2, 4 and 6
1.3 mm Defocused	Single	2, 4 and 6
1.0 mm Defocused	Multi	3
1.3 mm Defocused	Multi	3
1.0 mm Defocused	Multi	5
1.3 mm Defocused	Multi	5

3.4 CHARACTERISATIO AND ANALYSIS:

3.4.1 OPTICAL MICROSCOPE:

After laser treatment samples were grinded on belt grinder. In between grinding, sample kept cool by frequently dropping in water. This grinding was continued untill the surface was flat and free from nicks, burrs, etc., and all scratches were no longer visible. To see the microstructure polishing was done by emery paper from 0/0 to 4/0 followed by wheel polishing. Coarse alumina (~1mm), and fine alumina (~0.3 mm) suspension were used in subsequently. After that polishing sample was wash in running water. Dryer was used, for quick drying purposes. The polished face of the samples were etched using 3% Nital as an etchant to reveal the microstructures. Optical microscope was used for microstructure evolution. Hardness depth and width measured by reticule. Reticule is a graduated lens, used at a place of eyepiece. They were easily

rotated in any direction. By rotating in different direction, width and depth of the transformed region measured.

3.4.2 MICROHARDNESS TESTING:

Leitz miniload Microhardness tester was used for microhardness measurements. In this test, the instrument used squared-based diamond pyramid indenter with an inclined angle of 136^0 between opposite face, shown in fig. 3.4. Hardness of the transformed untransformed regions was measured by applying a load 5, 10, 15 and 25g. When these load were applied then square shape impressions obtain of the specimen surface. A microscope fitted with an ocular micrometer measured length of the diagonal of square, which contains movable knife-edges. Average diagonal was half of the sum of two diagonals. VHN was calculated using the formula,

$$VHN = 1.854\ P/\ d^2$$

where, P is the applied load in kg and d is the average diagonal of the indentation in mm. It provides a continuous scale of hardness of a given load, for soft materials it was 5VHN and for extremely hard materials 1500 VHN. Hardness of the different area was measured by moving the sample with screw gauge.

CHAPTER 4

RESULTS AND DISCUSSION

4.1 **Laser Hardening:**

First a proper size samples were cut from the Rail steel plate, afterwards grinding, polishing and etching was done in subsequent steps. The microstructure obtained by optical microscope shown in fig. 4.1. It was 100% pearlitic structure. Hence sample is 0.8% plane carbon steel. The effect of scanning speed and defocusing on the hardened dimension was studied. No hardening region obtained at scanning speeds higher than a certain values for fixed beam condition. Hence there was a limits of scanning speed within which hardening occurs for a fix power output. Beyond that limits no hardening occurs and below this speed fusion occurs near the surface. Fig. 4.2a shows this more clearly, at 2 mm/sce. scanning speed under focused beam condition groove form near the surface. Similarly no hardening was observed beyond certain defocusing at any speed. Because the temperature of the surface was below the critical temperature Ac_1. Hence surface layers did not reach in austenizing temperature range and no phase transformation occurs. Similar results were obtained by Ashby and Easterling [9] with hypoeutectiod steels having 0.1% C and 0.6%C.

It was very difficult to predict the exact focused position, therefor some experiments were done to decide the focused position, before the final experiment. Dimension analyses were done to decide the focused and defocused position. Accurate beam diameter measurement was not possible but relative focusing or defocusing diameter was easily obtained. First visually focusing the beam on the working sample surface and then defocused it by using screw gauge.

Three samples were scanned under focused laser beam and after that defocus the beam. By defocusing the beam various readings were taken. Optical microstructure was used for obtain the final microstructure. Width and depth of the transformed region was measured by "reticule". The depth and width of the hardened region, obtained by experiments has been listed in table 4.1. Fig 4.2 to 4.4 shows the effect of hardness

(a)

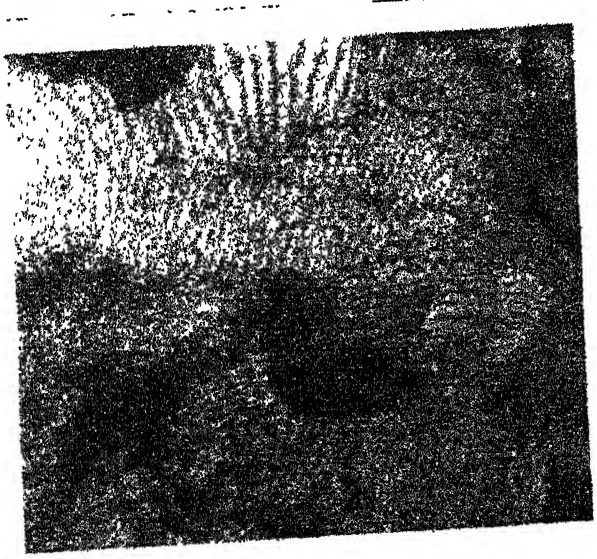

(b)

Fig. 4.1 Microstructure of the Eutectoid steel before hardening treatment

(a) 100 X (b)200 X

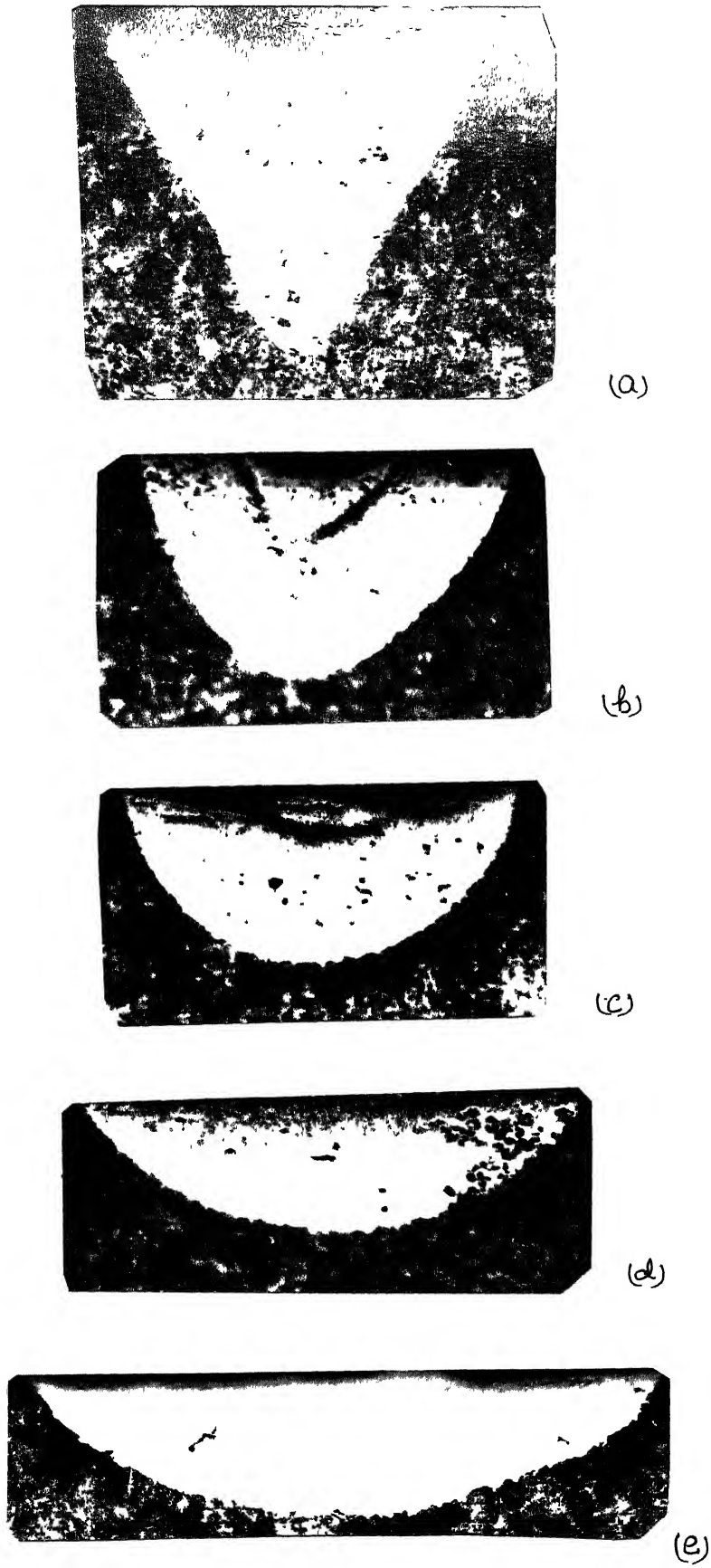

Fig. 4.2 Hardness depth profile of varies sample at 2 mm/ sec. Scanning speed.
(a) Focused beam (b) 0.3 mm Defocused (c) 0.7 mm Defocused
(d) 1.0 mm Defocused (e) 1.3 mm Defocused (50 X).

le 4.1 Varaition of depth and width of harden region in different scanning speed and beam condition.

(A) Scanning speed 2 mm/ sec.

Beam Condition	Width of the Harden region (mm)	Depth of the Harden region (mm)
Focused	0.90907	0.81815
0.3 mm Focused	0.97417	0.54643
0.7 mm Focused	0.96364	0.45452
1.0 mm Focused	1.0916	0.36371
1.3 mm Focused	1.1921	0.22724

(B) Scanning speed 4 mm/sec.

Beam Condition	Width of the Harden region(mm)	Depth of the Harden region (mm)
Focused	0.72731	0.54563
0.3 mm Focused	0.681817	0.36371
0.7 mm Focused	0.72741	0.3409
1.0 mm Focused	0.90907	0.2991
1.3 mm Focused	1.1362	0.236364

(C) Scanning speed 6 mm/sec.

Beam Condition	Width of the Harden region (mm)	Depth of the Harden region (mm)
Focused	0.45452	0.22727
0.3 mm Focused	0.65459	0.18181
0.7 mm Focused	0.7272	0.15912
1.0 mm Focused	0.36364	0.04545
1.3 mm Focused	Nil	Nil

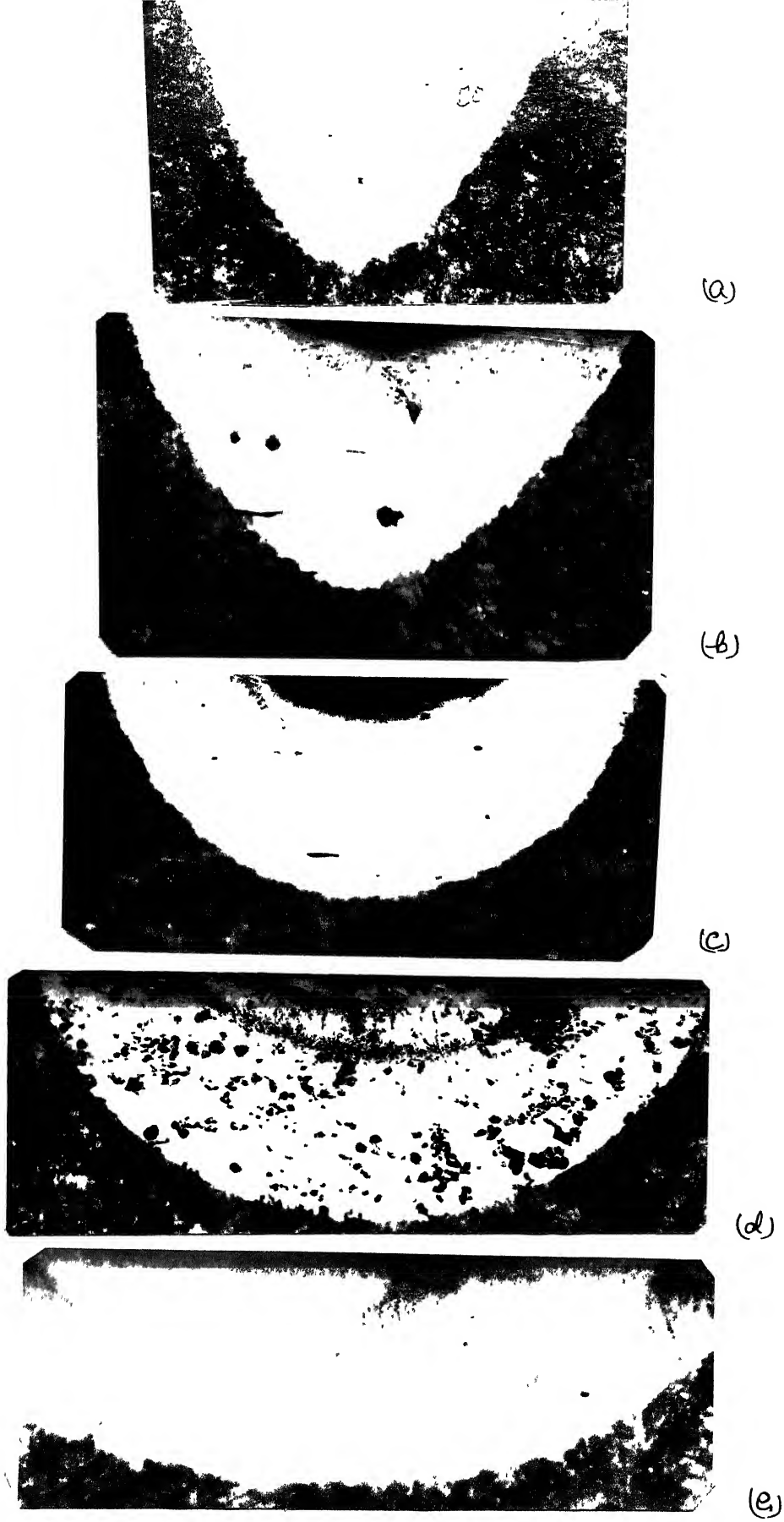

Fig. 4.3 Hardness depth profile of varies sample at 4 mm/ sec. Scanning speed.
(a) Focused beam (b) 0.3 mm Defocused (c) 0.7 mm Defocused
(d) 1.0 mm Defocused (e) 1.3 mm Defocused (100 X).

depth variation with scanning speed and beam condition. From this figure, it was observed that the hardened depth decreased, with increase in scan speed. In focused beam condition, depth was in the range of 0.23 to 0.8 mm, similar effect was observed by defocusing the beam at same scanning speed. When 4 mm/ sec. scanning speed was used then depth of harden in the range of 0.21 to 0.55 mm. But there was opposite effect of defocusing the laser beam on hardness width. The width of transformed region increased with defocusing the laser beam. It was observed that under all conditions the width of hardened region was more than the depth. Fig 4.2a to 4.2e shows this thing more clearly. If fusion (melting) was not occurs on the surface, than it was observed that there are negligible variations of hardness within the transformed region. The depth of hardness decreases as the scanning speed was increased, because the interaction time decrease and less energy absorbed. Defocusing the beam by small amount, it was absorbed that the depth of hardness decreases. This was happen because, the power density of the beam decrease. If defocused the laser beam upto 1.3-mm and using scanning velocity 6mm/sec., then there was no hardened region obtained. This happened, because interaction time was to much less. Fig. 4.5 shows the effect of interaction time on hardened region with same focused condition. As we know, interaction time depend upon scanning speed. Hence for obtaining the certain hardness depth, it is necessary to ensure a minimum interaction time. It shows that proper career should be required in between scanning speed and laser beam density.

Fig. 4.2(a to e) shows some typical structure of the hardened region, obtained by 2-mm/sec. scan speed in different beam condition. In this microstructure white region was observed as martensitic structure followed by pearlite (original structure). There was a sharp boundary in between transformed and untransformed region. Fig 4.3(a to e) and fig. 4.4 (a to e) shows the microstructure obtained by focused and defocused laser beam at higher speed i.e. 4 mm/sec. and 6 mm/sec. The microhardness of the hardened region was in the range of 950-970 VHN as compared to untreated (pearlite) region ~340-350 VHN.

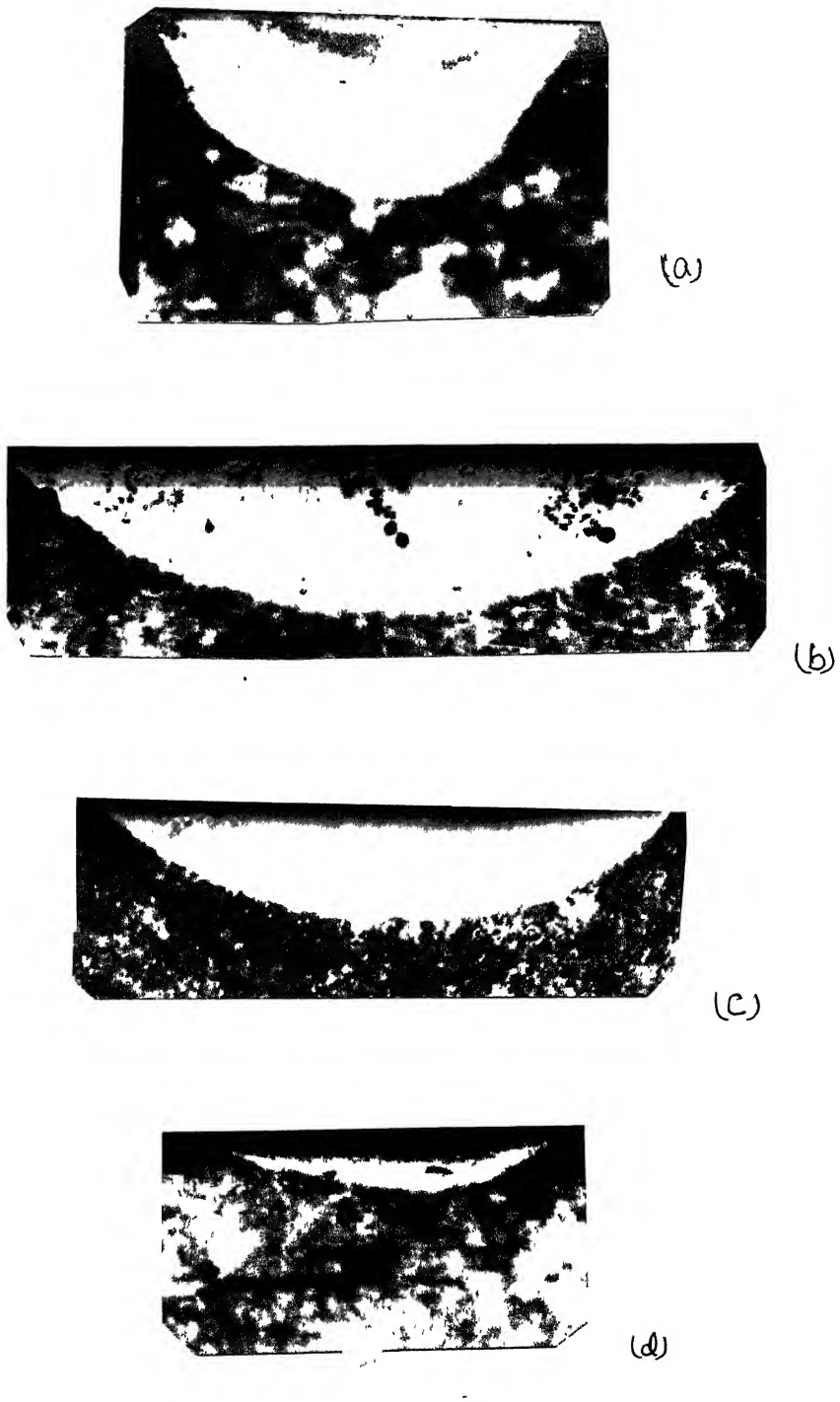

Fig. 4.4 Hardness depth profile of varies sample at 6 mm/ sec. Scanning speed.
(a) Focused beam (b) 0.3 mm Defocused (c) 0.7 mm Defocused
(d) 1.0 mm Defocused (100 X).

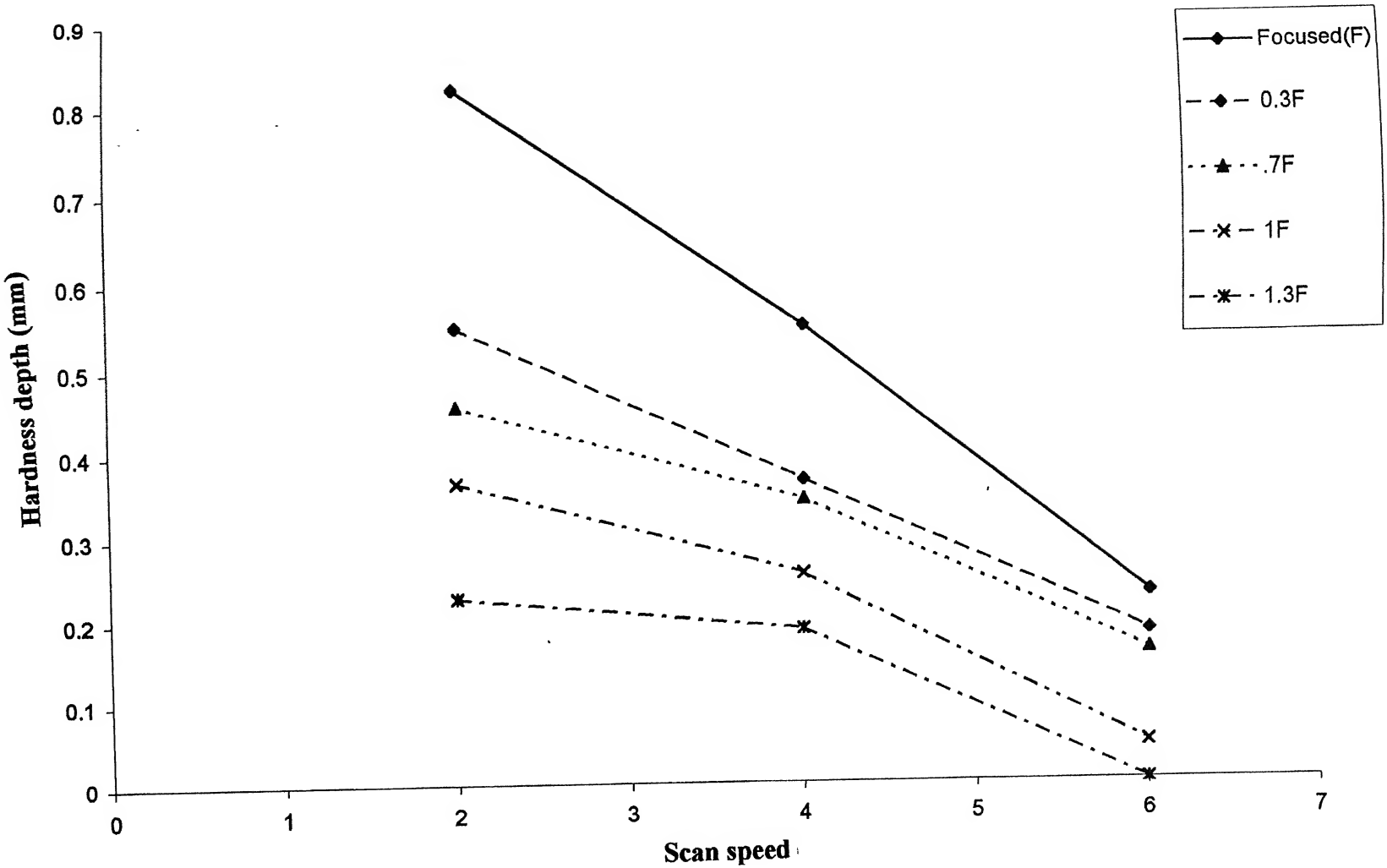

Fig. 4.5. Hardness variation with scanning speed form surface for focused laser beam condition.

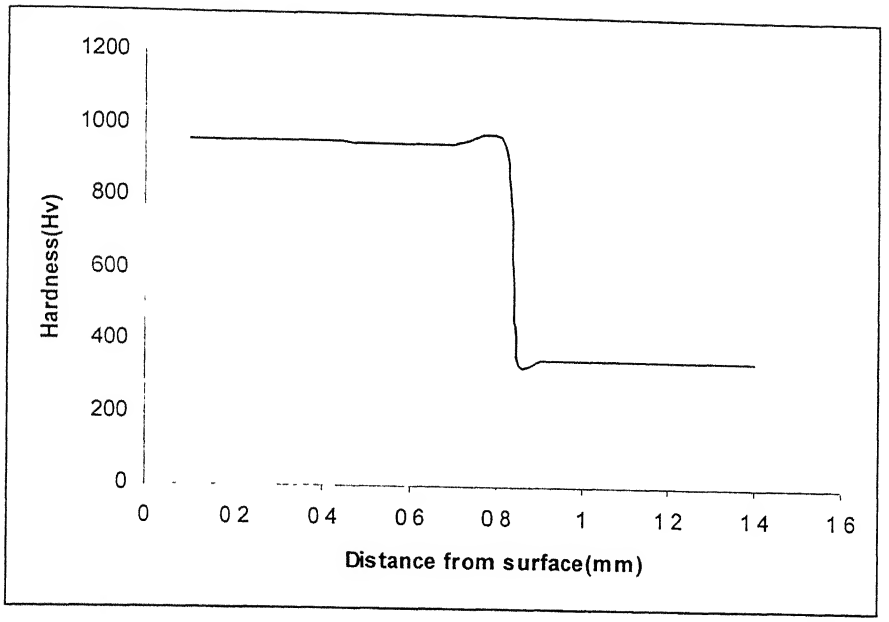

Fig. 4.6a : Hardness variation from surface for focused beam sample (2 mm /sec.)

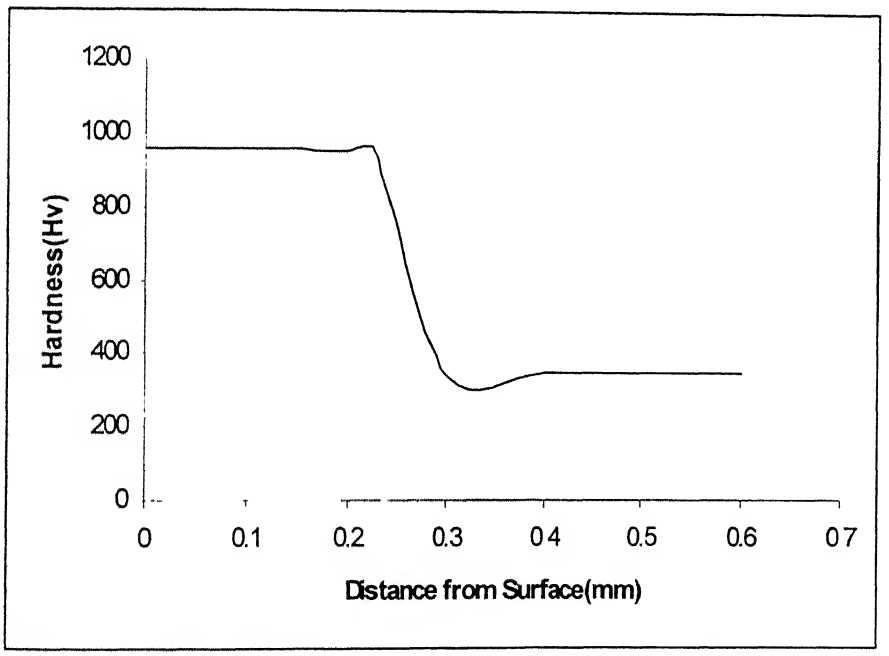

Fig. 4.6b: Hardness variation from surface for 1.3 mm defocused beam sample(2 mm /sec.)

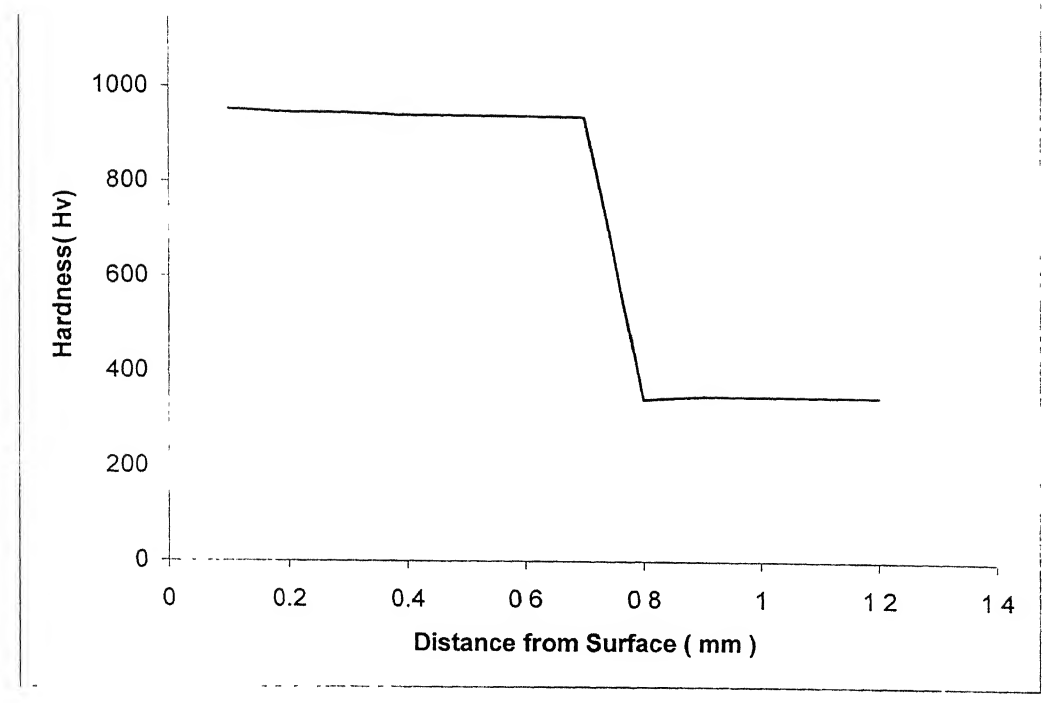

Fig. 4.7a : Hardness variation from surface for focused beam sample(4 mm /sec.)

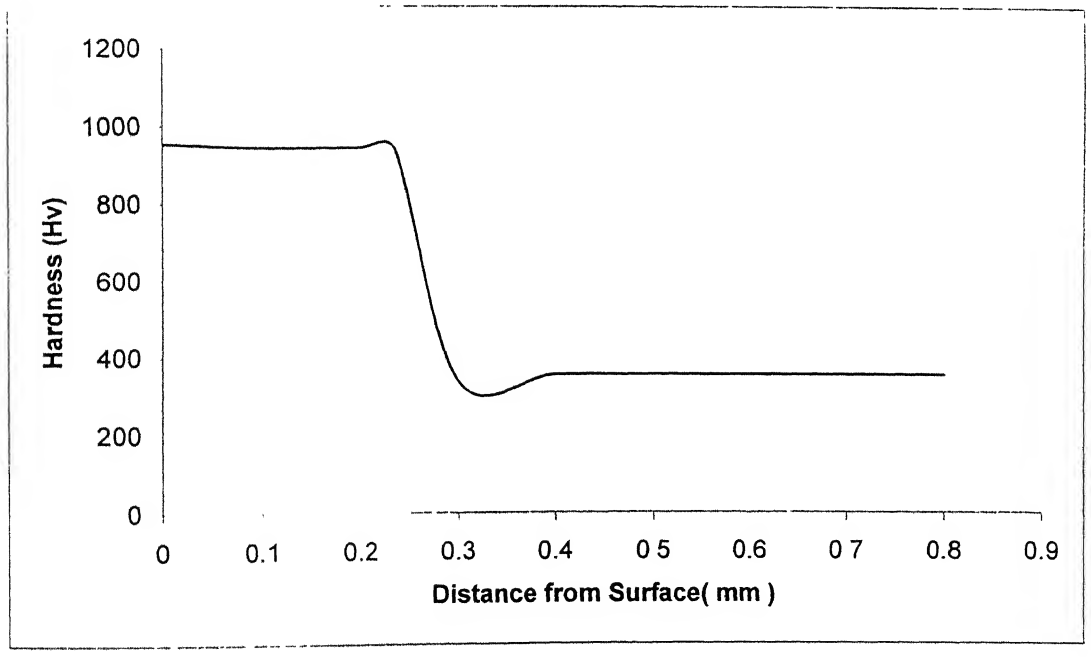

Fig. 4.7 b: Hardness variation from surface for 1.3mm defocused sample(4 mm /sec.)

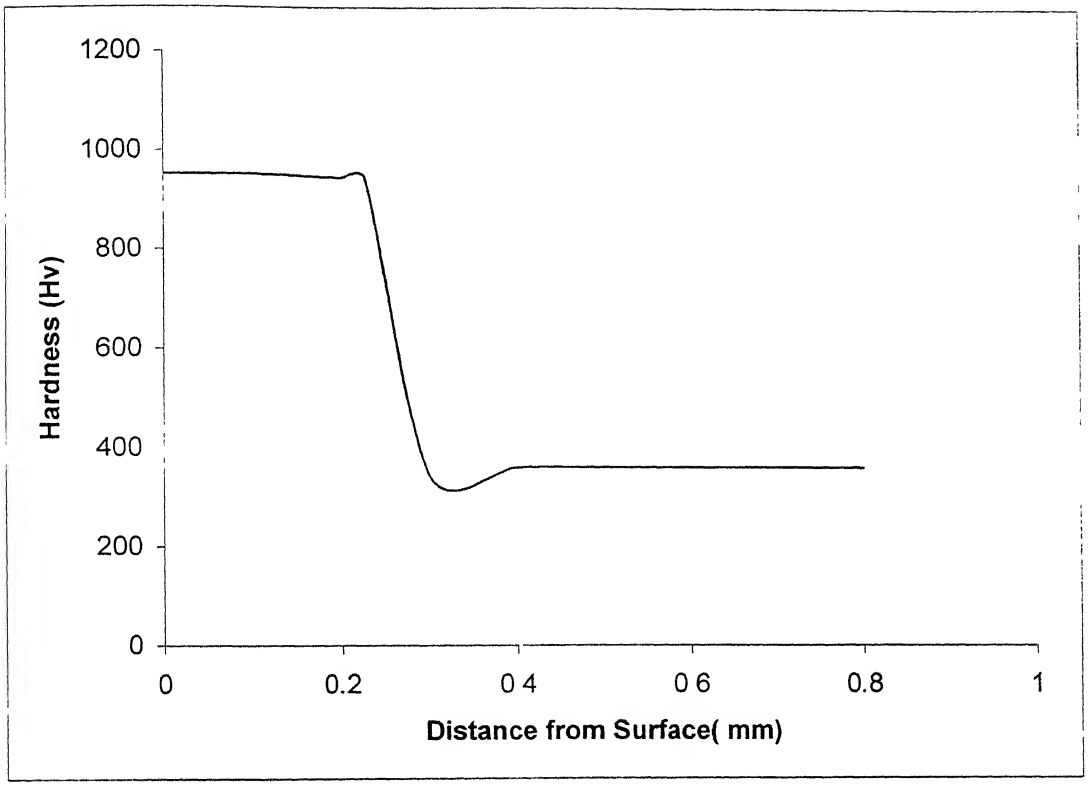

Fig. 4.8a : Hardness variation from surface for focused beam sample (6 mm /sec.)

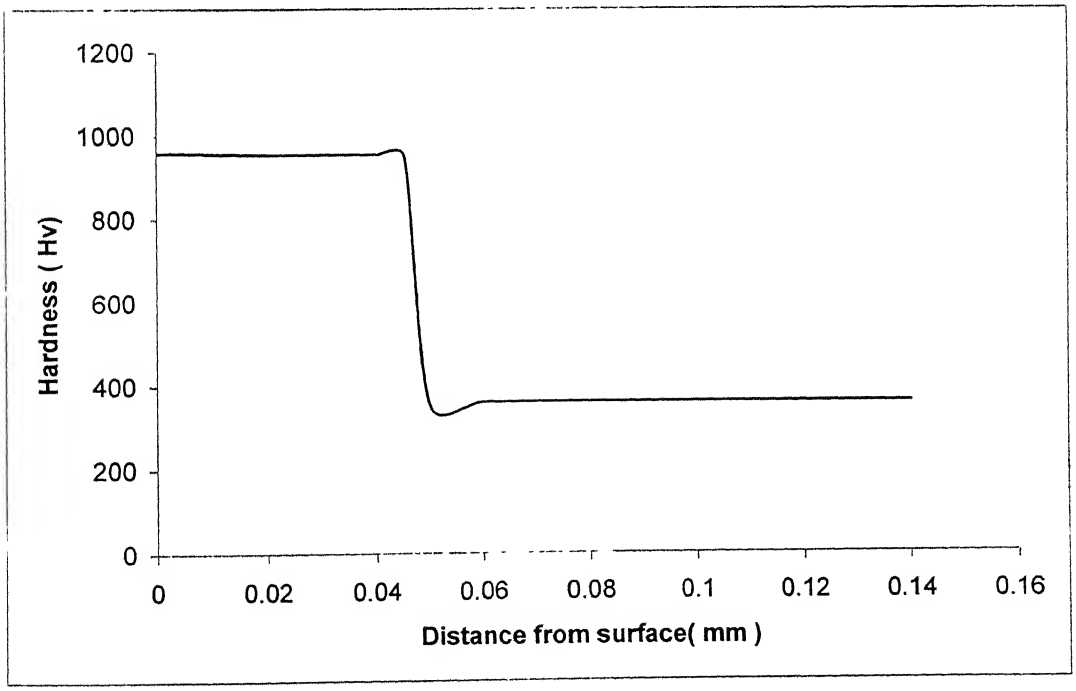

Fig. 4.8b: Hardness variation from surface for1 mm defocused beam sample(6mm /sec.).

Fig. 4.12 shows comparison the hardness depth obtained during experiments and theoretical values Theoretical depth calculated by following equation [3], which in he short form of the solution of the equation (6) and (7),

$$h\ (mm) = -0.11 + 3.02P / \sqrt{D_b V} \qquad (4.1)$$

where, D_b= Incident beam diameter (mm), P= laser power (KW), V= traverse speed (mm/sec.) and h is depth of hardening in mm. Incident diameter of the focused laser beam was calculated by D= f. R, where D is the diameter of the laser beam, f is the focal length of lens and R is the radiance of lens. Beam diameter for defocused condition was calculated by similar triangle method, shown in fig.4.17. Equation (4.1) gives the direct relation in between hardness depth with laser power, beam diameter and scanning speed. Fig. 4.12 shows, how hardness depth was varies with defocusing. Point near the curves indicates, observed hardness depth during experiments. At lower scan speed and focused beam condition, there was more difference in the observed and theoretical values. These differences obtained, because of high absorpvity (A) of laser beam by metal surface, which is used in equation 4.1. So at lower scan speed groove form near the surface. Above equation 4.1 is only applied for non-melting and groove free surface. Hence there was a difference in the observed and theoretical values. On the other points due to high absorption value, observed depth was slightly more then the theoretical depth.

4.2 **Microhardness Analysis:**

Microhardness of original matrix was ~ 350 Hv. The hardness value obtained after the laser treatment was analyzed by microhardness (Leitz) tester.

Fig 4.6 shows the microhardness profile of sample for scanning speed 2 mm / sec. .It was observed that under the focused beam condition some grove from near the surface. But these difficulties were removed, when defocused the beam. Hardness of the transferred region in which melting not occurs was ~ 950Hv. Near the boundary

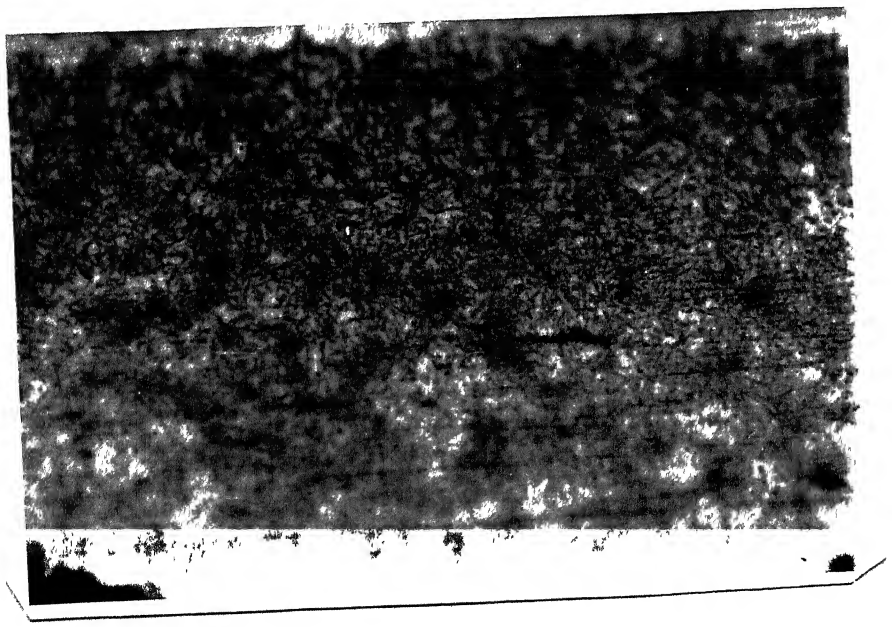

Fig. 4.9 Microstructure developed after hardening treatment.(200 X)

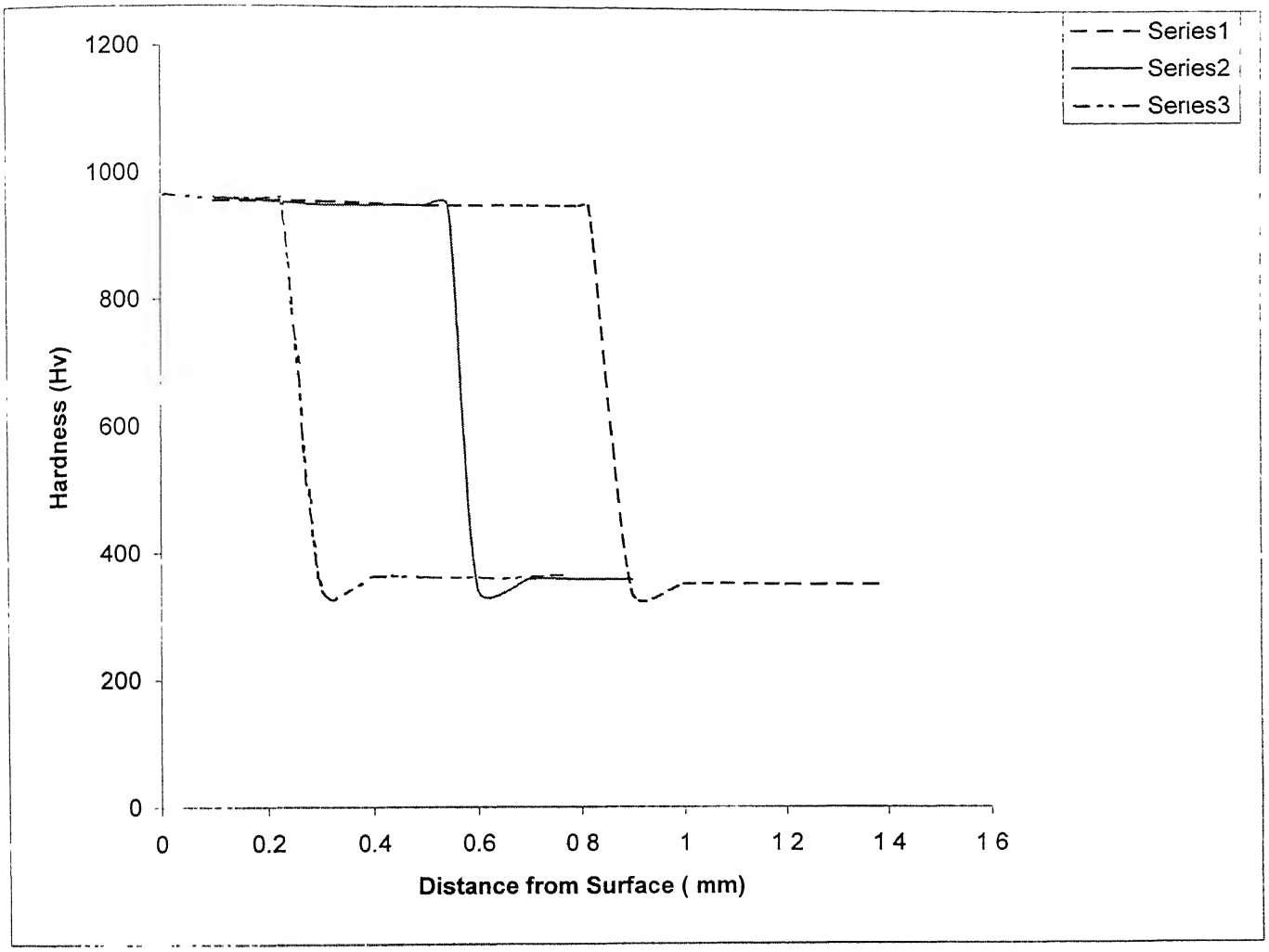

Fig. 4.10 : Hardness variation with scanning speed from surface for the focused laser beam sample.

Series1----2 mm/sec.
Series 2--- 4 mm/sec.
Series 3--- 6mm/sec.

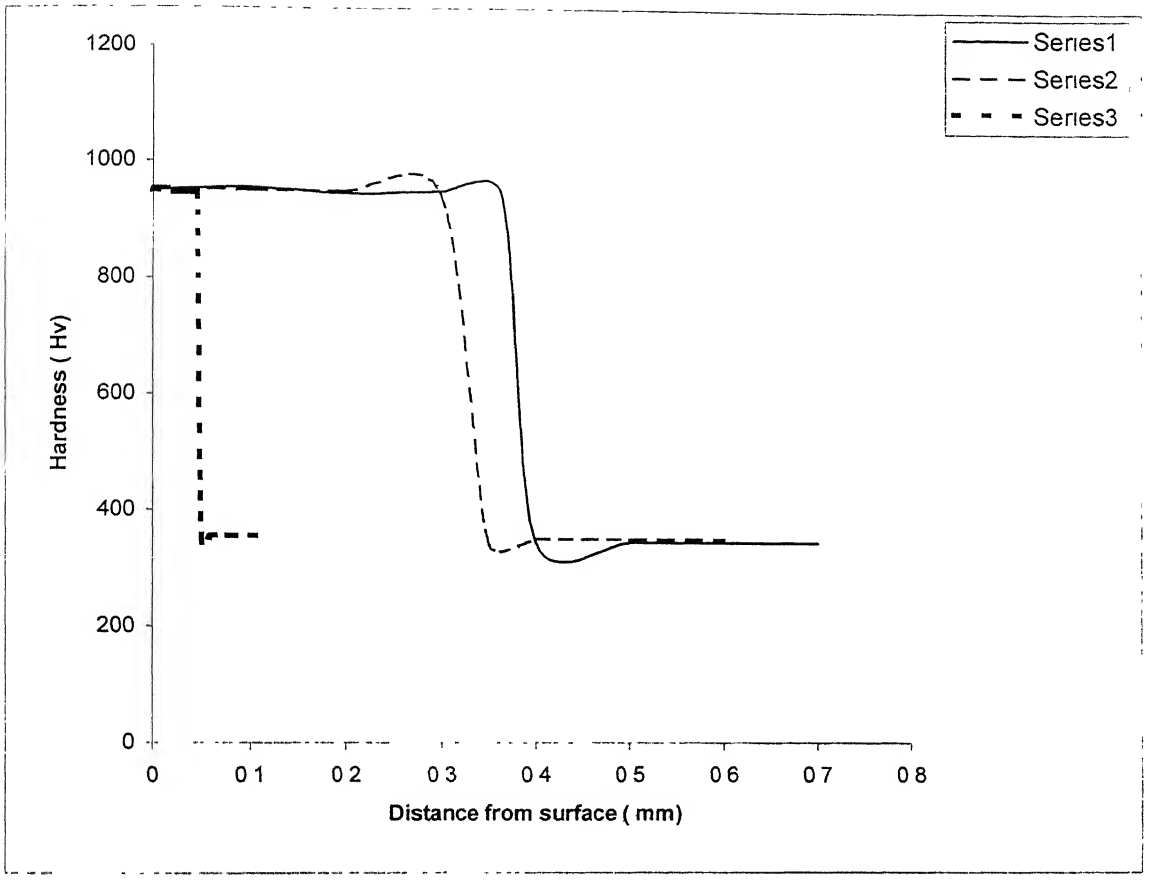

Fig. 4.11: Hardness variation with scanning speed form surface for 1mm defocused laser beam sample.

Series1--- 2 mm/ sec.

Series 2--- 4 mm / sec.

Series 3--- 6 mm / sec.

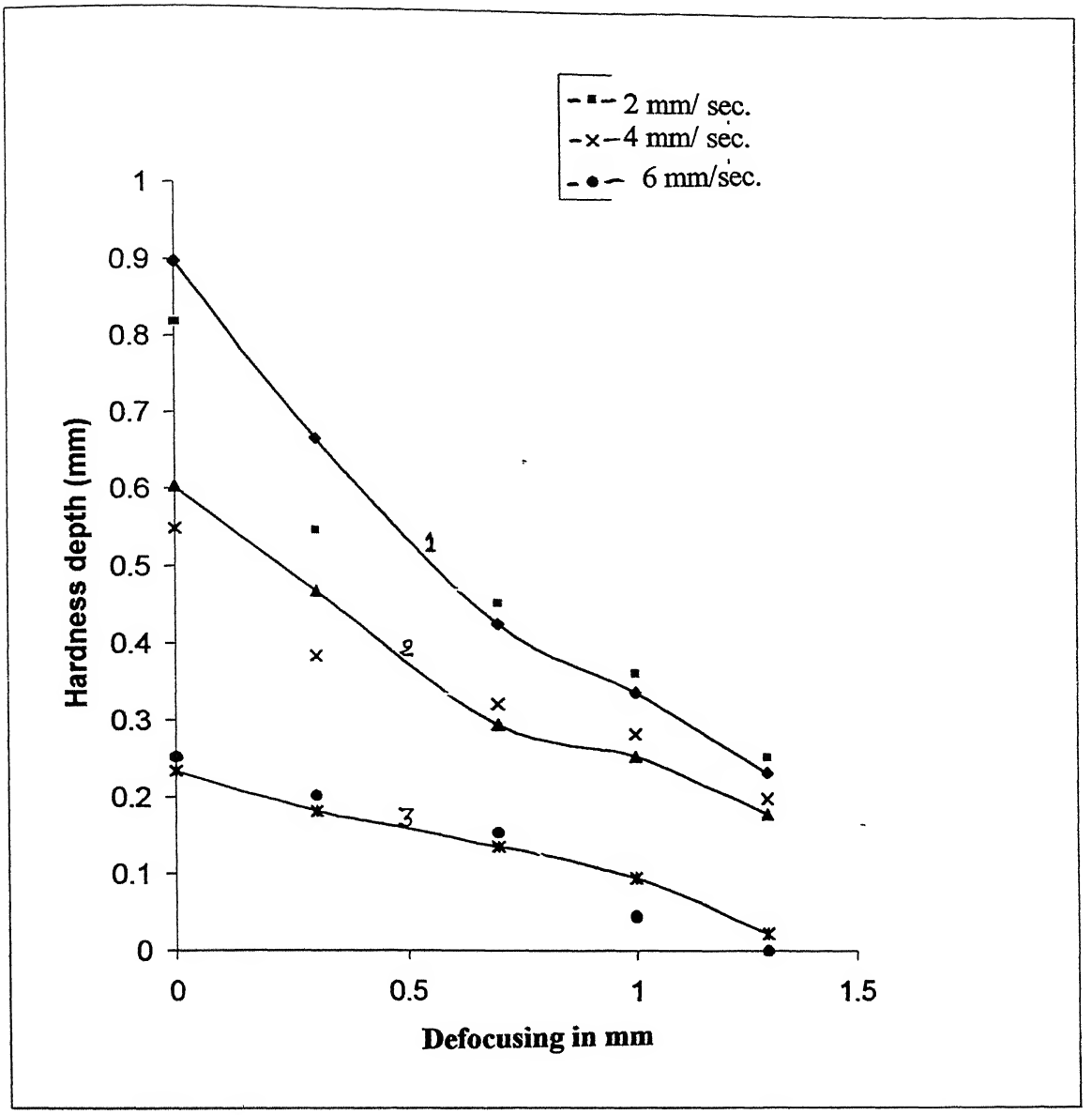

Fig. 4.12 Theoretical and Experimental hardness depth at different scan speed
(1) At 2 mm/ sec (2) At 4 mm/ sec. (3) At 6 mm/ sec.

between transformed and untransformed region the hardness value obtained slightly. lower ~ 330 Hv. Then there was a gradual increase in the hardness value till reaching the matrix hardness of 350 Hv. These shows, in this way the surface hardness increased nearly 2.7-3 times of original matrix. This much hardness obtained in transformed region, due to nearly all pearlite converted into martensite. Fig. 4.9 shows the martensitic structure within the transformed region. Due to high cooling rate there was no retain austenite in the transformed region. So laser treatment gives more hard surface compare to conventional treatment. By adjusting the various parameters groove free hard surface can be obtained. Fig 4.6(a to e) shows that when high scanning speed was used than no groove form near the surface. In this case hardness was obtained from surface i.e. no groove was formed. Similar hardness profiles were obtained by Kou, Sun and Lu [10] with 4140 steel. Meijer et al [13] got similar profile when studying laser-hardening effect on C45 steel.

Fig. 4.10 shows a comparison of hardness profiles of three samples, under same focused condition but different scanning speed. The hardness depth for 2 mm / sec. scanning speed was ~ 0.81 mm, where for 6 mm / sec. it was ~ 0.31 mm. The comparison clearly shows that the lesser the scanning speed more is the hardening depth. Same conclusion was drawn by Kou and Sun [11], while working on laser hardening effect on 4140 steel.

Fig. 4.11 compare of hardness profile under it defocused condition, but different scanning speed. This shows when we defocused the laser beam upto 1mm and use scanning speed 6 mm /sec., then obtained lesser hardness depth region ~ 0.042 mm. But within the transformed region, there was on variation of hardness value.

4.3 **Continuous Surface Hardening:**

By using a single hardened track, only certain width of the working sample was hard. But in real life, to make the whole surface of the specimen hard with laser heat treatment. Hence to obtain continuous hard surface, overlapping of the single hardened track was done. In the first set of experiment it was observed that the width of the hardened region was nearly 1mm in defocused condition. Hence to make the surface

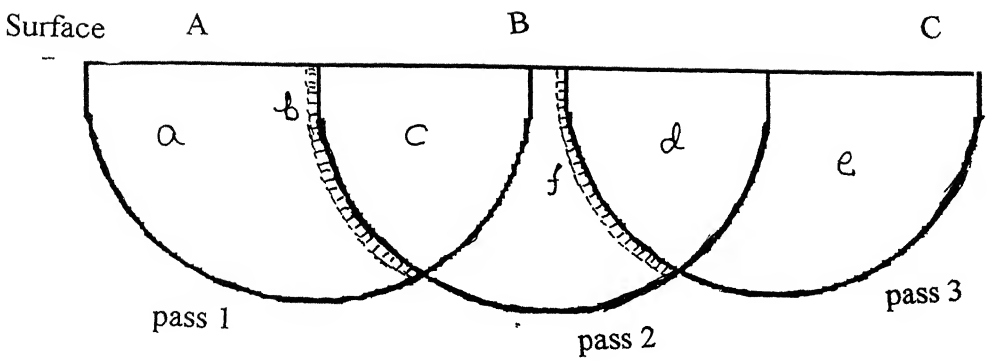

Fig 4.13 Schematic diagram to explain the effect of overlapping.

Table 4.2 Hardness depth of overlapped region on varies Scanning Speed and beam condition.

Scanning Speed	Beam Condition	Depth of Hardening (mm)
3 mm / sec.	1 mm Focused	0.2513
3 mm / sec.	1.3 mm Focused	0.1853
5 mm / sec.	1 mm Focused	0.2234
5 mm / sec.	1.3 mm Focused	0.1235

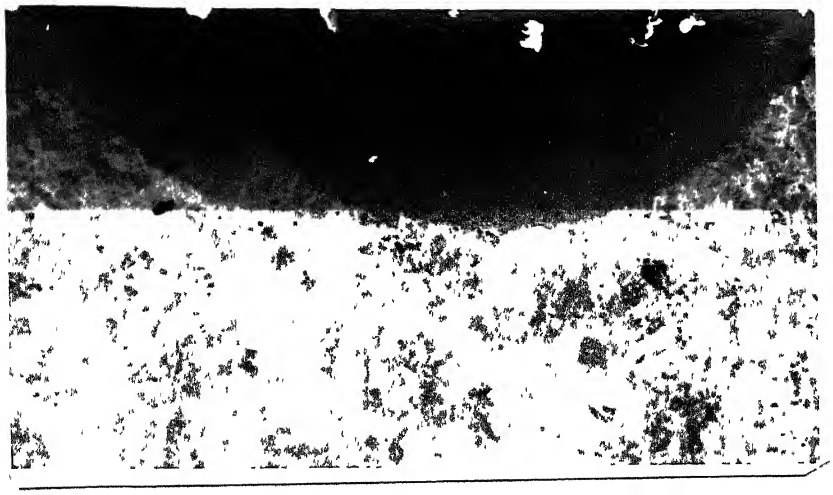

Fig. 4.14a Microstructure of overlapped region at scan speed 3mm/ sec. in 1mm defocused beam condition(200X).

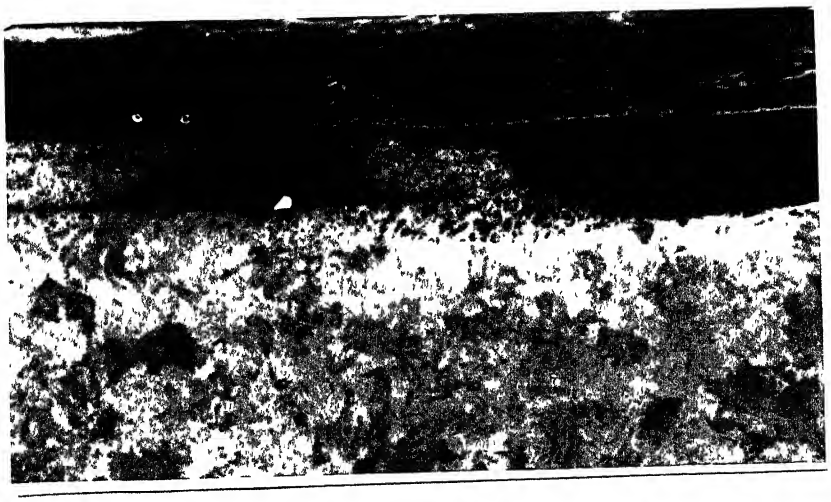

Fig. 4.14b Microstructure of continuous harden region at scan speed 3 mm/ sec.(100X)

Fig. 4.15a Microstructure of overlapped region at scan speed 5mm/ sec. in 1mm defocused beam condition(100X).

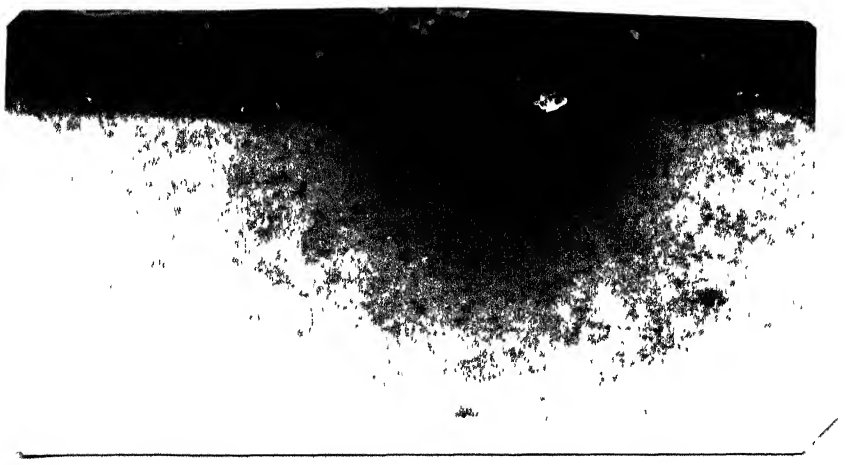

Fig. 4.15b Microstructure of continuous harden region at scan speed 5 mm/ sec.(100X)

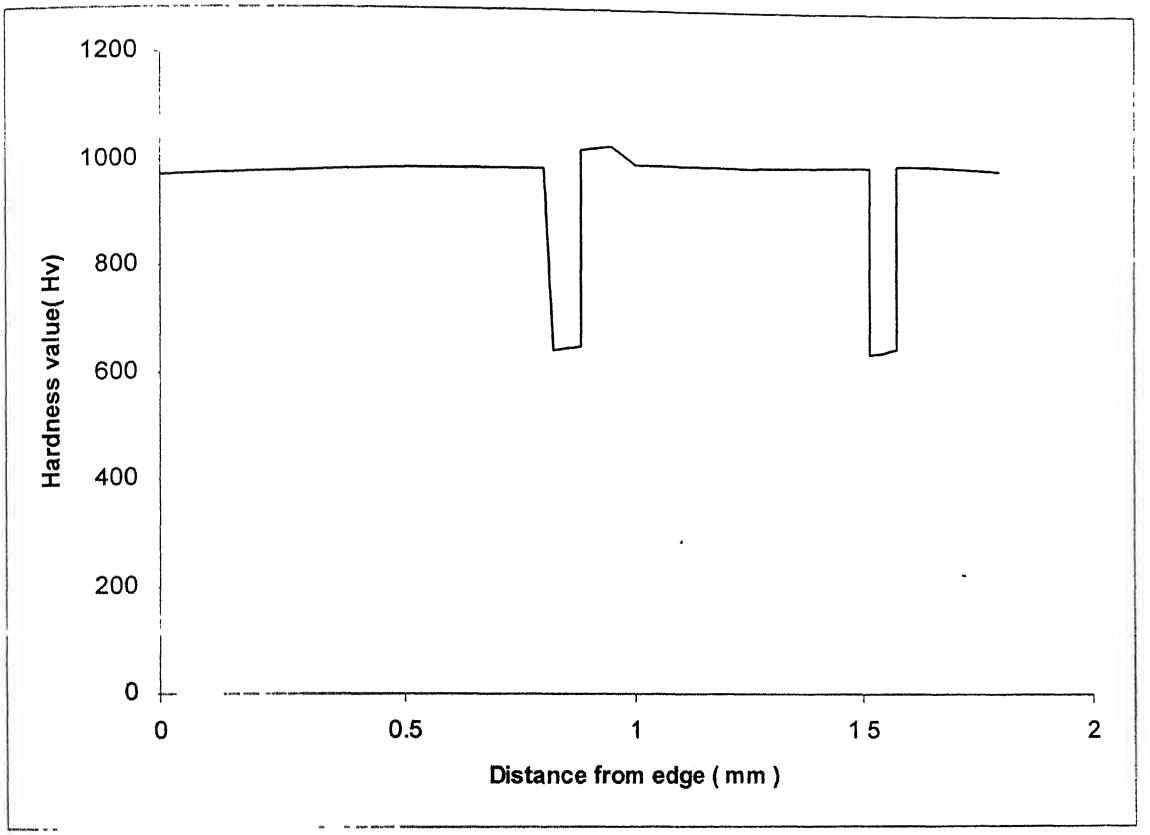

Fig. 4.16: Variation of Hardness along overlapped region.

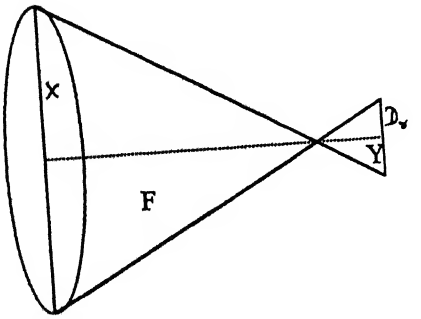

$$Y/X = D_r/F \quad \Rightarrow \quad D_r = (Y/X).\ F$$

Where, D_r is the real beam diameter, F =focal length of lens.
X = radius of lens, Y = Defocused distance

Fig. 4.17 Schematic Diagram for Defocused beam.

uniform harden, traveling the working sample by 0.5-mm distance between two passes normal to the scanning direction. Different experiment was done to see the effect of continuous surface hardness on working sample. It was observed that, if focused laser beam were used then surface burned and some groove was formed on the surface. Hence defocused laser beam used for this purpose. The width of the hardened region varies according to defocusing. Nearly fixed parameter used for 5-6 passes, so that a set of continuous hardened overlapped region can be obtained. Microhardness testing were done to know the variation of hardness within the transformed region. Table 4.2 shows the average depth of hardening of overlapped hardened region and fig 4.14 shows the overlapped hardened region.

Microstructural examination shows that the hardened region microstructures are not identical. Because it consists of martensite and tempered martensite in varying extent. So the microhardness of this region also varies, fig. 4.15 shows overlapped regions. This occurs because during continuous hardening, heating is done in already hardened region (Martensitic region). Hence some region get heated to the austenetic range and transformed to martensite during subsequent cooling. However the small region near to overlapped region will be heated to higher temperature (400- 500^{0}C) but did not reached in austenitic temperature range. Hence this region gets tempered and its hardness was lesser than the previous one. Microstructure and hardness across the overlapped region are shown in figure 4.12. A, B and C represents the three single laser treatment region, separated by 100 μm. Small regions like a, b, c, d, e and f was effected by the overlapping. In this diagram region c and d is completely overlapped and "a" and "e" are not overlapped. In this overlapping process, hatched region represented by "b" and " f" was effected. This region gets tempered during continuous hardening process. Because, the temperature of the region reached upto 400 - 500^{0}C, but not go in austenetic range. Hence the martensite tempered and losses there hardness upto ~ 630 Hv. Due to this tempering effect, there was variation of hardness in the tempered region. But there was no effect on the untempered region. Fig. 4.16 shows the variation of hardness along the width of the hardness region.

CONCLUSIONS

In this work surface hardening of eutectoid steel was done by using a 150-Watt CW laser. The effect of the scanning speed and beam diameter conditions on the laser hardening process had been studied. Continuous hard surface was obtained by overlapping of single track harden region. On the basis of the result obtained from the study, following conclusions can be drawn.

1. Maximum hardness achieved by laser hardening process was found to be higher than the hardness values achieved by conventional methods. The average hardness value of the hardened zone was ~ 950Hv
2. Depth and width of the hardened zone varied with laser parameters. Depth of hardened zone decreases, with the increase in scanning speed at fixed beam condition and increases the extent of defocusing. In the present work, hardening depth was in the range of 0.04mm to 0.8mm.
3. For a fixed power density the depth of transformed harden region increases with decrease in scanning speed as the interaction time increases. At lower scanning speed and focused beam condition groove formed near the surface.
4. No harden region was obtained, beyond a certain limit of defocusing at any speed. Hence at fixed scanning speed, there was certain range of beam defocusing beyond that on hardening occurs.
5. To obtain continuous hardness surface, overlapping of single hardened track was done. Keeping other variables fixed but shifts the sample by certain distance. Next to the overlapped regions, there was some decrease in hardness within the transformed regions. This variation was due to the tempering of martensite in heat- effected regions.

REFERENCES

1. Alexander A.Grigoryants, Basic of laser material processing, Mir publisher Moscow 1994.
2. Svelto Orazia and Hanna D.C, Principle of lasers (3 rd edition), plenum publishing corporation.
3. Singh Vijendra, Heat treatment of metals, Standard publishers distributor, Delhi 1998.
4. Bradley J.R and Kim S, Met. Trans. A, Vol.19A (1998) PP 2013-1025.
5. Prokhorov A.M, Konov V.I, Ursu I and Mihailescu I.N, Laser heating of metals, Adam Hilger.
6. Chryssoluris George, Laser machining theory and practice, Springer-Vergler.
7. Kykalin N, Uglov A and Kokora A, Laser maching and welding, Mir publications, Moscow 1987.
8. Lakhtin Y, Engg. Physical Metallurgy, Mir Publishers, Moscow, 1977.
9. Ashby M.F. and Easterling K.E., Acta. Metall., vol.32A, (1984) pp 1935-1948.
10. Kou S., Sun D.K., and Le Y.P., Met. Trans. A, Vol. 14A, 1983, pp 643-653.
11. Kou S., and Sun D.K., Met. Trans. A, Vol. 14A, 1983, pp1859-1867.
12. Kurz W., Giovanola B. and Trivedi R., Acta. Met., Vol.34, 1986, pp 823-830.
13. Meijer J., Seegers M., Vroegop P.H., and Wes G.J.N., Line hardening by low power CO_2 lasers, Pub. Kempston, IFS Kempston,1986.
14. Chan .C, Mazumder. J, and Chan. M.M, Met. Trans. 15A, 84, PP 2175- 2185.
15. Chande . T, and Mazumder. J, Appl. Phys. Lett.(41), 82, pp 42-48.
16. Bradley. J. R. and Kim. Sooho, Met. Trans. 19A, 1988, PP 2013-2025.

17 Zacharia . T, David S.A., Vitek J.M., and Debroy T., Met. Trans., 1989, pp 957- 966.

18 Zimmermann M., Carrard M., and Kurz W., Acta Metall., vol. 37, 1989, pp 3305-3315.

19 Bano N., Project report, Surface hardening of an eutectoid steel by 70-Watt laser. IIT Kanpur, 1998.

20 Kou S., and Wang Y.H., Met. Trans A, Vol. 17A, 1986, PP 2265-2269.

21 Mukherjee J., and Mazumdar J., Proc. The Metallurgical society of AIME, 1981, pp 221-245.

22 Rajan T.V., Sharma C.P., and Sharma A., Heat treatment principle and techniques, Prentice Hall of India Private Limited (seven edition) 1997.

23 Avner S.H., Introduction to Physical Metallurgy, McGraw-Hill Book Co.

24 Farias D., Denis S., and Simon A., Surface Engineering with high-energy beams, Trans. Tech. Publications, 1988, pp 139-152.

25 Kusinski J., Met. Trans. A, Vol. 19A, 1988, pp 377-381.

26 Merlin J., Oliviera C., and Li J.C., Surface Engineering with high energy beams, Trans. Tech. Publications, 1989, pp 175-188.

.....	.....
.....	.....
.....	.....
.....	.....
.....	.....
.....	.....
.....	.....
.....	.....
.....	.....
.....	.....
.....	.....